Check for updates

MR. BERNHARD KRATZER (Orcid ID : 0000-0003-1091-4327)
PROF. RUDOLF VALENTA (Orcid ID : 0000-0001-5944-3365)
PROF. WINFRIED F PICKL (Orcid ID : 0000-0003-0430-4952)

Article type : Original Article: Basic and Translational Allergy Immunology

Immunological imprint of COVID-19 on human peripheral blood leukocyte populations

Running title: Imprint of mild COVID-19 on the cellular immune system

Bernhard Kratzer[1], Doris Trapin[1], Paul Ettel[1], Ulrike Körmoczi[1], Arno Rottal[1], Friedrich Tuppy[1], Melanie Feichter[1], Pia Gattinger[2], Kristina Borochova[2], Yulia Dorofeeva[2], Inna Tulaeva[2, 3], Milena Weber[2], Katharina Grabmeier-Pfistershammer[1], Peter Tauber[1], Marika Gerdov[4], Bernhard Mühl[5], Thomas Perkmann[4], Ingrid Fae[6], Sabine Wenda[6], Harald Führer[7], Rainer Henning[8], Rudolf Valenta[2, 3, 9, 10, *] and Winfried F. Pickl[1, *]

[1]Institute of Immunology, Center for Pathophysiology, Infectiology and Immunology, Medical University of Vienna, Vienna, Austria.
[2]Institute of Pathophysiology and Allergy Research, Center for Pathophysiology, Infectiology and Immunology, Medical University of Vienna, Vienna, Austria.
[3]Laboratory for Immunopathology, Department of Clinical Immunology and Allergology, I. M. Sechenov First Moscow State Medical University (Sechenov University), Moscow, Russia.
[4]Department of Laboratory Medicine, Medical University of Vienna, Vienna, Austria.
[5]Labors.at, Vienna, Austria.

This article has been accepted for publication and undergone full peer review but has not been through the copyediting, typesetting, pagination and proofreading process, which may lead to differences between this version and the Version of Record. Please cite this article as doi: 10.1111/ALL.14647

This article is protected by copyright. All rights reserved

Accepted Article

[6] Department for Blood Group Serology and Transfusion Medicine, Medical University of Vienna, Vienna, Austria.
[7]Statistical Consultants, Vienna, Austria.
[8]Viravaxx, Vienna, Austria.
[9]NRC Institute of Immunology FMBA of Russia, Moscow, Russia.
[10]Karl Landsteiner University of Health Sciences, Krems, Austria.

word count abstract: 248
word count text: 4.651

***) Corresponding authors:**
Winfried F. Pickl, MD
Institute of Immunology, Center for Pathophysiology, Infectiology and Immunology,
Medical University of Vienna, Lazarettgasse 19, 1090 Vienna, Austria.
Phone: (+431) 40160 33245.
Fax: (+431) 40160 933245.
Email: winfried.pickl@meduniwien.ac.at.
ORCID ID: orcid.org/0000-0003-0430-4952
&
Rudolf Valenta
Department of Pathophysiology and Allergy Research
Medical University of Vienna
Waehringer Guertel 18-20
A-1090 Vienna, Austria
Tel: (+431) 40400 51080
Fax: (+431) 40400 51300
E-mail: rudolf.valenta@meduniwien.ac.at
ORCID ID: 0000-0001-5944-3365

Accepted Article

This article is protected by copyright. All rights reserved

Author contributions

B. K., R. V. and W. F. P. designed research; B. K., D. T., P. E., U. K., A. R., F. T., M. F., P. G., K. B., Y. D., I. T., M. W., K. G.-P., P. T., M.G., B. M., T. P. I. F., S. W., H. F., R. H., R. V., W. F. P., performed research and analyzed data; B. K., R. V., and W. F. P., wrote the paper. All authors critically read the paper and approved the manuscript.

Conflict of interest disclosures

With regards to the authors disclosure of potential conflicts of interest we would like to indicate that Winfried F. Pickl holds stocks of Biomay AG and has received honoraria from Novartis, Astra Zeneca and Roche. Rudolf Valenta has received research grants from HVD Life-Sciences, Vienna, Austria, and from Viravaxx, Vienna, Austria. He serves as consultant for Viravaxx. The other authors have no conflict of interest to declare. Rainer Henning is an employee of Viravaxx, Vienna, Austria.

Accepted Article

This article is protected by copyright. All rights reserved

Accepted Article

ABSTRACT

Background: SARS-CoV-2 has triggered a pandemic that is now claiming many lives. Several studies have investigated cellular immune responses in COVID-19 patients during disease but little is known regarding a possible protracted impact of COVID-19 on the adaptive and innate immune system in COVID-19-convalescent patients.

Methods: We used multiparametric flow cytometry to analyze whole peripheral blood samples, and determined SARS-CoV-2 specific antibody levels against the S-protein, its RBD-subunit and viral nucleocapsid in a cohort of COVID-19 convalescent patients who had mild disease approximately 10 weeks after infection (n=109) and healthy control subjects (n=98). Furthermore, we correlated immunological changes with clinical and demographic parameters.

Results: Even ten weeks after disease COVID-19 convalescent patients had fewer neutrophils, while their cytotoxic $CD8^+$ T cells were activated, reflected as higher HLA-DR and CD38 expression. Multiparametric regression analyses showed that in COVID-19 patients both $CD3^+CD4^+$ and $CD3^+CD8^+$ effector memory cells were higher, while $CD25^+Foxp3^+$ T regulatory cells were lower. In addition, both transitional B cell and plasmablast levels were significantly elevated in COVID-19 patients. Fever (duration, level) correlated with numbers of central memory $CD4^+$ T cells and anti-S and anti-RBD, but not anti-NC antibody levels. Moreover, a "young immunological age" as determined by numbers of $CD3^+CD45RA^+CD62L^+CD31^+$ recent thymic emigrants was associated with a loss of sense of taste and/or smell.

Conclusion: Acute SARS-CoV-2 infection leaves protracted beneficial (i.e., activation of T cells) and potentially harmful (i.e., reduction of neutrophils) imprints in the cellular immune system in addition to induction of specific antibody responses.

This article is protected by copyright. All rights reserved

Key words: SARS-CoV, COVID, T cells, lymphocytes, flow cytometry, infections, B cells, clinical immunology,

Abbreviations:

ACE2: angiotensin converting enzyme 2
CD: cluster of differentiation
CoV-2: coronavirus 2
COVID-19: coronavirus disease 2019
EBV: Epstein-Barr virus
ELISA: enzyme-linked immunosorbent assay
HC: healthy control
HLA: human leukocyte antigen
HRP: horseradish peroxidase
Ig: immunoglobulin
KREC: kappa-deleting recombination excision circles
MERS: Middle East respiratory syndrome
NC: nucleocapsid
OD: optical density
PB: peripheral blood
PBMC: peripheral blood mononuclear cells
PCA: principal component analysis
RBD: receptor-binding domain
RTE: recent thymic emigrant T cells
rtPCR: reverse transcription polymerase chain reaction
S: spike protein
SARS: severe acute respiratory syndrome
TRAC: T cell receptor alpha chain
TREC: T cell receptor excision circles

This article is protected by copyright. All rights reserved

INTRODUCTION

An outbreak of an epidemic respiratory infection that caused severe pneumonia in a subgroup of patients was reported in December 2019 in Wuhan City, Hubei Province, China [1-3]. Shortly thereafter, it was shown that the disease was caused by a novel beta coronavirus (CoV) subsequently called SARS-CoV-2 [4], and the respiratory disease caused by this virus was named COVID-19 [5,6]. Similar to SARS-CoV, SARS-CoV-2 binds with the receptor-binding domain (RBD) of its spike(S)-protein to and enters the target cells via the angiotensin converting enzyme 2 (ACE2) receptor [7-9], however, alternative receptors for cell entry such as CD147/EMMPRIN/Basigin [10] and CD299 (formerly CD209L) may exist [11,12]. SARS-CoV-2 is highly infectious and is easily spread by aerosols [13,14].

Accordingly, since December 2019 and until September 15, 2020, SARS-CoV-2 has infected 29,281,638 people worldwide and caused 928,423 deaths, representing a mortality rate of 3.44%. Austria has been similarly affected by the pandemic, with 33,541infected persons and 757 deaths to date (https://coronavirus.jhu.edu/map.html).

Current data indicate a long and relatively mild initial course of the disease after SARS-CoV-2 infection, which may be followed by a severe course after a median time of 8 days from the first symptoms. The mild period may be followed by a period of breathlessness (approximately on day 8), which may turn into acute respiratory distress syndrome (ARDS) on day 9, followed by admission to intensive care on day 10.5 [15-17] Acute infection with SARS-CoV-2 can be proven by detecting nucleic acids from the virus in nasopharyngeal swabs or lavages [18]. After the acute infection, SARS-CoV-2-specific antibodies [9,16] are usually formed, which coincides with the clearance of the virus from the body and a delayed response might be associated with mortality [19]. However, SARS-CoV-2-specific antibodies have varying specificities and titers for different antigens/epitopes and it has been shown that antibodies from convalescents after a mild COVID-19 infection cannot always prevent the virus from binding to ACE2 and may therefore not have a protective effect [9].

Similarly, several studies have investigated the effect(s) of a primary SARS-CoV-2 infection on leukocyte populations in the body in general, and on T and B lymphocyte

This article is protected by copyright. All rights reserved

subsets in particular. Also the SARS-CoV-2-specific T cell response has been investigated by several research groups [17,20-29].

Notably, memory CD4+ T cells have been suggested to mediate protective immunity against the previously circulating CoV-strains SARS-CoV [30] and MERS [31], respectively, and CD8+ memory T cell responses have been observed in SARS-CoV convalescent patients years after primary infection [32]. However, regarding infection with the novel coronavirus SARS-CoV-2 recent reports have revealed conflicting results with one study (analyzing PB lymphocyte subsets in 44 patients) pointing towards reduced T memory and T regulatory cell populations in severe COVID-19 patients, suggesting that immune dysregulation potentially leads to aggravated inflammatory responses in patients [28]. In contrast, another study provided evidence for segregation between memory T cells from patients with acute severe or acute moderate COVID-19 disease and the development of memory T cells from recently convalescent individuals (42-58 days after infection) and healthy controls [33]. The latter study found only very moderate changes in a group of 40 COVID-19 convalescent patients who underwent a mild COVID-19 disease course (49-64 days after disease onset).
However, the available studies on cellular immune responses were mainly conducted patients suffering from COVID-19 but little is known about the protracted effects of COVID-19 on cellular immune responses. There is a need for systematic studies analyzing COVID-19 effects on cellular immune responses in cohorts of well documented COVID-19 convalescent patients, in particular, for those who had experienced mild disease constituting the majority of cases, to understand if and how the infection continues to stimulate and/or perturb the immune system of the convalescent host. It is also unclear how possible changes in peripheral leukocyte/lymphocyte compartments correlate with SARS-CoV-2 specific antibody levels and/or clinical symptoms.

Accordingly, the aims of this study were to identify the immunological imprint of primary COVID-19 infection on peripheral blood (PB) cell populations and antibody levels. We were especially interested whether distinct changes in blood cell or antibody parameters would separate COVID-19 convalescent patients from healthy subjects and whether we could define parameters which may be associated with the disease course, disease

This article is protected by copyright. All rights reserved

duration, preexisting medical conditions, regular medications or demographic parameters. Thus we performed here a systematic study to investigate the distribution of leukocyte subsets in peripheral blood with a special interest in T and B lymphocyte subpopulations of COVID-19 convalescent patients 10 weeks after mild SARS-CoV-2 infection and compared results with a large, age matched, healthy control group, which was recruited in parallel and was negative for SARS-CoV-2 antibodies and had a negative SARS-Cov2 rtPCR at the time of venipuncture. Therefore, and in order to unequivocally determine leukocyte, T and B lymphocyte populations we performed whole-blood multiparametric flow cytometry on COVID-19 patient and control peripheral blood (PB) samples. Furthermore, we determined SARS-CoV-2 specific antibody levels against S-protein, its subunit the RBD-protein and the viral nucleocapsid and analyzed whether thymic and/or bone marrow output were affected in COVID-19 patients who underwent a mild disease course.

Accepted Article

This article is protected by copyright. All rights reserved

Accepted Article

MATERIALS AND METHODS

Patients, control subjects and trial conduct

Between May 11, 2020 and July 2, 2020, 109 patients diagnosed with COVID-19 disease 10 weeks previously (71.2±16.5 days) were enrolled into this study. The 109 patients had rtPCR-confirmed (n=92, 84.4%) and/or SARS-CoV-2 antibody-confirmed (Elecsys® Anti-SARS-CoV-2 assay Roche) (n=108 tested, n=107 positive, 99.1%) COVID-19 disease [34]. In parallel, 98 healthy control subjects, who were reportedly asymptomatic for the last 10 weeks and who were SARS-CoV-2 negative by certified SARS-CoV-2 antibody test (Elecsys® Anti-SARS-CoV-2 assay Roche) and had a negative rtPCR test for SARS-CoV-2 at the time of venipuncture were enrolled into the study. Similar to the COVID-19 patients also the HC collective had different co-morbidities as specified in Table 1. All patients gave their written informed consent in accordance with the Declaration of Helsinki. The study was approved by the Ethics Committee of the Medical University of Vienna (EK No.: 1302/2020). Venous blood was drawn from all subjects and was either EDTA-anticoagulated (for flow cytometric analyses and determination of lymphocyte emigration rates from thymus using TREC and KREC technology), heparin-anticoagulated (for cryopreservation of PBMC), or silicon dioxide coagulated (to obtain serum for determining specific antibodies).

Immunophenotyping by multiparametric flow cytometry

Immunophenotyping was performed by using optimal concentrations of directly conjugated monoclonal antibodies (**Supplemental Table S1**) to leukocyte and lymphocyte (sub)populations according to standard quality controlled (inter-laboratory test validated) procedures [35].

Additional methods can be found in the Appendix 1 in the online repository to this article.

This article is protected by copyright. All rights reserved

RESULTS

Clinical characterization of COVID-19 convalescent patients.

Between May 11, 2020 and July 2, 2020, 109 COVID-19 convalescent patients and 98 healthy control subjects were enrolled into this retrospective study. The group of COVID-19 convalescent patients and the group of healthy control subjects was well balanced regarding gender, age, height and weight (**Table 1**). COVID-19 convalescent patients were studied approximately 10 weeks after disease and healthy control subjects had no symptoms indicative of COVID-19 or a common cold 10 weeks before participating in the study. COVID-19 convalescent patients analyzed in this study (n=109) consisted of 61 males and 48 females with a median age of 52 years (range 16-78), and a mean COVID-19 disease duration of 15.5±13.5 days (range, 0-66 days). The COVID-19 disease symptoms in convalescent patients started 10 weeks (71.2±16.5 (mean±SD) days) before venipuncture/enrollment into this study. Seventy-seven percent of patients presented with elevated body temperature (**Table 1**) for 4.3±4.8 days with a median body temperature of 38.5 °C (range 37.1-42.0), 55% of patients had fever (>38 °C). The most frequent clinical symptoms (**Table 1**) were fatigue (84.4%), followed by cough (69.7%), loss of taste or smell (66.1%), headache (66.1%), myalgia (51.4%), arthralgia (50.5%), chills or rigor (49.5%), nasal congestion (43.1%), shortness of breath (42.2%) and sore throat (38.5%). Gastrointestinal symptoms were much less frequently observed with diarrhea (27.5%), nausea (20.2%) and vomiting (6.4%). Of the 109 COVID-19 patients in this cohort only eight (7.3%) had to be hospitalized for a mean of 5.9±5.8 days, with three patients requiring non-invasive O_2-therapy. At the time of venipuncture, patients were symptom free for 55.3±18.0 days. Seventy-one patients (65.1%) had a preexisting health condition, while forty-nine patients (45%) took regular medications (**Table S2**). None of the patients was pregnant, 6.4% of patients reported to be smokers and 37.6% of patients reported to drink alcohol on a recreational basis.

The control group consisted of healthy subjects (**Table 1**), who did not have COVID-19 associated disease symptoms for the last 70 days before venipuncture. Control subjects were enrolled and analyzed in parallel to the COVID-19 convalescent patients and consisted of 98 individuals, 44 males (44.9%) and 54 females (55.1%) with a median age of 51 years (range 14-77). Per definition, all subjects within the control group had a

This article is protected by copyright. All rights reserved

negative rtPCR test at the time of venipuncture and all tested negative with a certified commercial SARS-CoV-2 antibody test (Elecsys® Anti-SARS-CoV-2 assay, Roche).

Primary SARS-CoV-2 infection induces protracted reduction of neutrophil counts and reveals increased numbers of activated cytotoxic T cells in the circulation.

First, we determined overall peripheral blood (PB) leukocyte subpopulations in the COVID-19 patient collective and in healthy control subjects. Remarkably, the COVID-19 convalescent patients showed significantly less leukocytes compared to the healthy control subjects (6384±1677 x 10^6/L versus 7006±1961 x 10^6/L; p=0.0156), which was due to highly significantly lower neutrophil counts (4111±1477 x 10^6/L versus 4693±1588 x 10^6/L; p=0.0041) (**Figure 1, Figure S1 and Table S3**). Neutropenia is frequently associated with trivial acute viral infections, but usually resolves after one week [36]. While all COVID-19 patients studied herein had rtPCR- and/or anti-SARS-CoV-2-confirmed COVID-19 disease, possible co-infections with other viruses at the time of COVID-19 infection cannot be excluded. Due to the enormous case-load of PCR tests in the period March-May, i.e., when the first wave of the COVID-19 pandemic was at its peak in Austria, no capacity for addition PCR-tests was available, which represents a limitation of this study.

In contrast to neutrophils, numbers of monocytes, $CD3^+$ T cells, irrespective whether TCR alpha/$beta^+$ or TCR gamma/$delta^+$, similar to the $CD3^+CD4^+$ and $CD3^+CD8^+$ T cell subsets, $CD56^+$ NK cells and $CD19^+$ B cells did not reveal significant differences between COVID-19 convalescent patients and healthy control individuals (**Figure 1 and Table S3**). However, $CD3^+$ T cells of COVID-19 convalescent patients showed distinct signs of activation, with significantly more $CD3^+$ T cells expressing HLA-DR on their surface (107±85 x 10^6/L versus 81±54 x 10^6/L, p=0.0248; 5.78±3.84% versus 4.34±2.50%; p=0.0054) (**Table S3**). That HLA-DR is a well-known activation antigen of human T lymphocytes [37] which is also associated with acute viral infections [38,39] has been described previously. T cell subset analyses revealed that the subset of cytotoxic $CD3^+CD8^+$ T cells exclusively accounted for that difference (61±65 x 10^6/L versus 38±34 x 10^6/L; p=0.0079; 3.21±2.91% versus 2.05±1.61%; p=0.014), while $CD3^+CD4^+$ T cells

This article is protected by copyright. All rights reserved

had no increased signs of activation when compared for HLA-DR expression to those of healthy controls (33±18 x 10^6/L versus 31±19 x 10^6/L; p=0.3630) (**Figure 1 and Figure S2**). Activation of the T cell compartment in COVID-19 convalescent patients was also evident when we examined CD38 co-expression on $CD3^+$ T cells (4.6±3.6 x 10^6/L versus 3.5±2.7 x 10^6/L; p=0.0275; 0.27±0.24% versus 0.19±0.14%, p=0.0051), which is another important activation antigen and also an endothelial adhesion molecule known for its upregulation on virus-specific T cells [38,39]. Notably, and in clear contrast to HLA-DR expression which was restricted to $CD3^+CD8^+$ T cells, significant up-regulation of CD38 on lymphocytes of COVID-19 convalescent patients was observed on both, $CD4^+$ and $CD8^+$ T cells (**Table S3**).

Numbers of naïve and effector memory $CD3^+CD4^+$ T helper cells and effector memory $CD3^+CD8^+$ cytotoxic T cells are higher in the blood of COVID-19 convalescent patients compared to healthy controls.

Notably, a dramatic increase of the subset of $CD3^+CD4^+$ T cells co-expressing the high affinity IL-7 receptor alpha chain (CD127) irrespective of the presence (137±114 x 10^6/L versus 79±106 x 10^6/L, p<0.0001; 24.47±13.68% versus 15.66±13.79%, p<0.0001) or absence (498±226 x 10^6/L versus 370±248 x 10^6/L; p<0.0001; 62.44±17.69% versus 44.83±24.22%, p<0.0001) of CD45RA co-expression and marking naïve and effector memory $CD3^+CD4^+$ T helper cells, respectively, was found (**Figures 2, S3, S4A and Table S4**). This dramatic expansion appeared to be at the expense of $Foxp3^+CD25^+CD127^-CD3^+CD4^+$ T regulatory cells, which were significantly reduced in patients compared to healthy controls (11±15 x 10^6/L versus 15±11 x 10^6/L, p=0.0004; 27.73±25.70% versus 42.10±27.26%, p=0.0001) (**Table S4**).

Apart from the clear-cut expansion of naïve and effector $CD4^+$ T helper cells, significantly more $CD3^+CD8^+CD45RO^+CD45RA^-$ memory T cells were present in the blood of COVID-19 convalescent patients as compared to healthy controls (113±79 x 10^6/L versus 87±54 x 10^6/L; p=0.0263) (**Figures 2, S4B**), which was also reflected by their significantly higher relative levels among $CD3^+$ T cells (8.58±4.67% versus 6.82±3.88%; p<0.0045) (**Supplemental Table S4**). The elevated levels of memory T cells almost exclusively belonged to the $CD45RO^+CCR7^-$ effector memory subset (128±89 x 10^6/L versus 99±55 x 10^6/L; p=0.0502), which was significantly higher among $CD3^+CD8^+$ T cells

This article is protected by copyright. All rights reserved

(32.42±14.65% versus 26.90±11.11%; p=0.0052), while this was not evident for the central memory subset of $CD3^+CD8^+CD45RO^+CCR7^+$ (15±14 versus 15±10 10^6/L; p=0.7532) (**Figures 2, S3**). Although $CD3^+CD8^+$ effector memory cells mostly belonged to the subset of early effector cells as defined by their co-expression of CD27 and CD28 [40], COVID-19 convalescent patients had a significantly lower frequency of this subset among their $CD3^+CD8^+CD45RO^+CCR7^-$ effector memory T cells (65.6±13.0 versus 69.7±13.0%, p=0.0129), which was at the expense of more differentiated $CD3^+CD8^+$ T effector memory subsets, *i.e.,* those co-expressing $CD27^+CD28^-$ and $CD27^-CD28^-$, respectively (**Figure S5**). Notably, higher numbers of $CD3^+CD8^+$ memory T cells were paralleled by a decrease in absolute (85±66 x 10^6/L versus 108±92 x 10^6/L; p=0.0704) and relative (21.52±13.91% versus 26.60±15.13%; p=0.0145) numbers of $CD3^+CD8^+CD45RO^-CCR7^+$ naïve cytotoxic T cells.

Moreover, moderately lower number of $CD3^+CD4^+CD45RA^+CD62L^+CD31^+$ recent thymic emigrant (RTE) cells (141±103 versus 165±126; p=0.2078; 17.01±10.85% versus 18.40±10.27%, p=0.2215) were observed. Similarly, relative (20.81±13.78% versus 23.73±16.64%; p=0.3592) and absolute (83±70 x 10^6/L versus 100±95 x 10^6/L; p=0.5770) amounts of $CD3^+CD8^+CD45RA^+CD62L^+CD31^+$ recent thymic emigrant T cells were lower, however, both changes did not reach statistical significance. The above findings may be indicative of decreased thymic output of both $CD4^+$ and $CD8^+$ T cells. However, determination of T cell receptor excision circles of PB T cells (TRECs), which negatively correlated with the increased age of our patients and correlated with the numbers of both $CD3^+CD4^+$ and $CD3^+CD8^+$ RTE did not indicate problems with thymic output in COVID-19 convalescent patients with a mild disease course when compared to healthy control subjects (**Figures 2, S3**).

Levels of transitional B cells and plasmablasts are higher in the blood of COVID-19 convalescent patients while B memory compartments are unaffected.

Next, we determined B cell subset distribution and found that major B cell subpopulations such as naïve B cells, non-class-switched and class-switched memory B cells were not different between COVID-19 convalescent patients and healthy control subjects (**Figures 3, S6, S7 and Table S5**). This finding was interesting, given the observed and above

This article is protected by copyright. All rights reserved

described gross distortions of T memory cell populations in COVID-19 convalescent patients. However, $CD19^+CD38^{high}IgM^+$ transitional B cells were significantly higher in COVID-19 convalescent patients when compared to healthy control subjects (4.98±3.10% versus 3.80±2.31%; p=0.0046) (**Figures 3, S6, S7 and Table S5**). Similarly, $CD19^+CD38^+IgM^-$ plasmablasts were both absolutely (2.4±1.7 x 10^6/L versus 1.8±1.5 x 10^6/L; p=0.0104) and relatively (1.56±0.99% versus 1.12±0.99%; p=0.0028) higher in COVID-19 patients as compared to healthy control subjects (**Figures 3, S6, S7 and Table S5**). That the current bone marrow output of B cell precursors was not depressed in COVID-19 convalescent patients could be demonstrated by determining kappa recombination excision circles (KRECs), which were not different from the healthy control population (**Figure 3**).

Multivariate logistic regression analyses confirm associations between COVID-19 disease and imprint on immune cell parameters.

In a next step, multivariate logistic regression analyses were performed for the 46 significant blood cell and serum parameters identified in univariate analyses. Receiver operating characteristic (ROC) curves (**Figure S8)** demonstrate that COVID-19 convalescent patients and HC subjects differ regarding several immune cell parameters. Indeed, elevated numbers of $CD3^+CD4^+CD45RA^+CD127^+$ naïve T helper cells (area under the curve (AUC) 66.2%; 95% confidence interval (CI) 58.1-74.3%; p<0.001) and of cytotoxic $CD3^+CD8^+CD45RO^+CCR7^-$ effector memory T cells (AUC 60.1%; 95% CI 51.8% to 68.5%; p=0.022) were clearly higher in COVID-19 convalescent individuals than HC. In contrast, relative numbers of $CD3^+CD4^+CD45RA^+Foxp3^+CD25^+CD127^-$ T regulatory cells (p=0.047) and of antigen-experienced(AE)3 cytotoxic $CD3^+CD8^+CD27^+CD28^-CD45RA^{+/-}$ T cells (p=0.012) were significantly lower in COVID-19 convalescent patients when compared to HC subjects. Moreover, both higher frequencies of transitional $CD19^+CD38^+IgM^{high}$ B cells (AUC 65.4%; 95% CI 57.4% to 73.5%; p<0.001) as well as $CD19^+CD38^+IgM^-$ plasmablasts (AUC 70.3%; 95% CI 62.3 to 78.2%; p<0.001) significantly discriminated COVID-19 convalescent individuals from HC.

Associations between clinical parameters and changes in blood cells and serum parameters

This article is protected by copyright. All rights reserved

Next, we performed univariate analyses in order to investigate whether blood cell parameters and/or SARS-CoV-2-specific antibody levels (S-, RBD- and NC-protein) would correlate with clinical symptoms (**Figure 4A**), co-morbidities and pre-medications of COVID-19 patients. Most notably, we found that convalescent patients who had more severe fever during their disease had significantly higher relative numbers of $CD3^+CD4^+CD45RO^+CCR7^+$ central memory helper T cells (**Figure 4B**) in their blood (p=0.0003). In addition, relative numbers of $CD3^+CD4^+CD45RO^+CCR7^+$ central memory helper T cells were significantly associated with chills (p=0.0030; data not shown), and with the number of fever days (p=0.0045; **Figure 4C**). These findings were corroborated by significant inverse correlations observed between highest fever and relative and absolute numbers of naïve $CD3^+CD4^+CD45RO^-CCR7^+$ T cells (p=0.0025 and p=0.0034, respectively; not shown). Notably, patients who had fever during their disease also presented with significantly more activated $CD19^+CD21^{low}CD38^{low}$ B cells [41] (**Figure 4D**; p=0.0045).

Moreover, the number of fever days and the presence of fever in general (not shown), correlated well with both the levels of anti-S-protein IgG (p=0.0002) and anti-RBD IgG (p=0.0166) as determined by ELISA (**Figure 4E and F**). In contrast, anti-NC antibodies only moderately correlated with fever/highest temperature (not shown) but not duration of fever (**Figure 4G**).

Another very interesting finding was the fact that patients suffering from loss of taste/smell had significantly more $CD3^+CD45RA^+CD62L^+CD31^+$RTEs in their blood (**Figure 4H**). While $CD3^+CD45RA^+CD62L^+CD31^+$ recent thymic emigrant cells positively correlate with TREC numbers (p<0.0001) and negatively with biological age (p<0.0001) this association was only evident when the age was determined “immunologically”, i.e., by multicolor flow cytometry but not upon determination of birth age. This finding may indicate that individuals with a “young(er) immune system” are more likely to suffer from loss of taste/smell when infected by SARS-CoV-2. That loss of taste/smell represents indeed a separate clinical factor in COVID-19 patients, which is clearly different from, e.g., the fever/coughing/fatigue- or the arthralgia/myalgia-factor was confirmed by principal component analysis (PCA), reducing clinical symptoms to factors best explaining the variance of variables, followed by rotated component matrix relation

This article is protected by copyright. All rights reserved

determination (Varimax-Rotation) using the collected clinical symptom categories (**Table 2**). These analyses revealed seven factors defined by certain symptoms (factor 1: fever, chills, rigor, fatigue, cough; factor 2: running nose, nasal congestion, sore throat, sneeze; factor 3: arthralgia, myalgia; factor 4: conjunctivitis, other GI problems; factor 5: pneumonia, shortness of breath, wheezing; factor 6: vomiting, nausea, headache, diarrhea; factor 7: other symptoms, loss of taste, smell) with an explained proportion of variance of 65.4% (KMO=0.728; Bartlett's test of sphericity $p<0.001$) and identified loss of taste/smell as a clearly separate clinical disease entity.

Not unexpectedly, the age of patients correlated with the prevalence of cardiovascular, metabolic and renal diseases in the COVID-19 convalescent patients, however, surprisingly not with disease duration and severity (fever days, fever height) although age is frequently associated with a higher mortality risk [42]. Notably, a total of 45% of COVID-19 convalescent patients took regular medications (**Table S2**) with 16 out of the 109 patients reporting intake of ACE- or angiotensin receptor (AT) blockers (candesartan, lisinopril, enalapril, ramipril, irbesartan, valsartan), i.e., substances which have been shown to lead to increased ACE2 receptor expression in cardiac tissue in preclinical models previously [43]. While ACE/AT inhibitor intake positively correlated with the age of patients ($p<0.0001$), it apparently did not correlate with the disease course, e. g., duration of fever ($p=0.7316$) or of clinical symptoms ($p=0.6131$). Of significance, also 11 subjects in the control group took ACE/AT inhibitors as regular medication, thus there was no significant difference between the patient and control group regarding ACE/AT inhibitor consumption.

This article is protected by copyright. All rights reserved

DISCUSSION

We here show that acute SARS-CoV-2 infection has protracted impacts on the human immune system even in COVID-19 convalescent patients who underwent a mild disease course. Our data support the view that SARS-CoV-2 challenges the human immune system at different levels. We show that even 70 days after acute SARS-CoV2 infection protracted reduction of neutrophil counts is observed in COVID-19 convalescent patients (n=109) when compared to healthy control subjects (n=98), which is paralleled by activation of T cells as demonstrated by higher HLA-DR ($CD8^+$ T cells) and CD38 ($CD4^+$ and $CD8^+$) expression. Moreover, significantly greater numbers of $CD3^+CD4^+CD127^+CD45RA^-$ effector memory T cells as well as of $CD3^+CD8^+CD45RO^+CCR7^-$ effector memory T cells clearly distinguished COVID-19 convalescent individuals from healthy control subjects. While both B memory cell populations (non-class switched and class switched) did not differ between COVID-19 convalescent patients and healthy control subjects, numbers of early B cells characterized as $CD19^+IgM^+CD38^+$ transitional B cells as well as plasmablasts were higher in convalescents as compared to healthy controls. Increased plasmablast levels had been reported in severe COVID-19 patients at the time of the disease previously [22]. SARS-CoV-2 specific antibody levels were detectable in all but one patient who had received chemotherapy. Interestingly, anti-S and anti-RBD antibody levels as well as $CD3^+CD8^+CD45RO^+CCR7^+$ central memory T cells, but not anti-nucleocapsid antibodies, correlated with duration of fever.

Virus-induced reduction of neutrophils is a common feature of childhood infections including respiratory syncytial virus (RSV), influenza A and B, and parvovirus. In most cases, neutropenia occurs during the first few days of viral illness and lasts for a maximum of eight days [36]. However, some viruses have been shown to be associated with decreased neutrophil numbers and even neutropenia, after the acute phase of infection, such as EBV [44], Hepatitis A virus [45], measles [46], varicella [47], phlebotomus fever virus (Sicilian type) [48] and rubella [49]. For the latter two viral infections reduced neutrophil counts are maintained for up to 6-weeks after initial infection. The mechanistic basis for the reduced neutrophil counts may be either complement-fixing anti-neutrophil antibodies or exhaustion of the neutrophil pool.

This article is protected by copyright. All rights reserved

Accepted Article

The observation that even 70 days after infection T cells are expressing HLA-DR and CD38 speaks for their sustained SARS-CoV-2 dependent activation. Indeed, HLA-DR becomes upregulated upon T cell activation [37] and has been demonstrated to be increased on $CD8^+$ cytotoxic T cells of patients suffering from autoimmune diseases [50] or acute and chronic viral infections such as HIV [51] [38,39] and also in the acute phase of COVID-19 [22,52]. What may be the function of increased HLA-DR surface expression on $CD8^+$ T cells? Notably, $HLA\text{-}DR^+$ cytotoxic T cells have been shown to possess all the requirements for processing and loading of antigens onto HLA-DR molecules [53]. Moreover, cytotoxic T cells are also proficient to express the canonical co-stimulatory molecules CD86 and CD80, which are essential for the priming and activation of effector T cells [53]. In addition, a previous report has shown that T cell-T cell synapses have a major role in the generation of protective $CD8^+$ T cell memory since conjugated cells critically polarize each other towards the secretion of interferon-gamma (IFN-gamma) [54].

We here also found increased CD38 expression on both $CD4^+$ and $CD8^+$ T cells of COVID-19 convalescent patients. In fact, CD38 (adenosine diphosphate (ADP) ribosyl cyclase) marks T cells with increased cytotoxic capability [38,39] and enhanced ability to produce cytokines [55]. Furthermore, CD38 endows T cells with improved interaction with endothelial cells via CD31 [56], which has been shown to lead to improved adhesion of lymphocytes to endothelium [57]. Whether this also leads to enhanced extravasation of T cells is an open question, but it is tempting to speculate that $CD38^+$ T cells might have an improved capability to target sites of inflammation.

Antibodies and T cells are the two main antigen-specific effector systems for resolving viral infections. Notably, both T cell subsets contribute to viral clearance [58,59]. In fact, anti-viral $CD4^+$ T cell responses are important for optimal antibody and $CD8^+$ T cell responses. Thus it is not entirely unexpected, that we found significantly elevated numbers of effector memory $CD4^+CD45RA^+CD127^+$ T cells in COVID-19 convalescent patients. What is, however, surprising is the level and degree of maintenance of these cells in patients with a mild COVID-19 disease course, because we could easily identify their high numbers even without applying antigen-specific detection methods such as

This article is protected by copyright. All rights reserved

tetramer-staining. One mechanism for the sustained expansion of these effector cells seems to be the mitigation of T regulatory responses, which is reflected by significantly lower $CD25^{+}Foxp3^{+}CD127^{-}$ T cells in convalescents as compared to healthy controls (**Figure 2** and **Table S4**)

Whether the $CD4^{+}$ effector cells have mere helper function for the clonal expansion of the SARS-CoV-2-specific B cells or may also exert cytotoxic cellular programs remains to be shown in future analyses. Nevertheless, besides the expanded $CD4^{+}$ T cells, we also detected a significant expansion of the $CD8^{+}$ effector memory pool. These cells are supposedly cytotoxic and well-apt to attack and lyse SARS-CoV-2-infected cells. They also contribute to the activated $CD8^{+}$ T cell pool found elevated in convalescents, which co-expresses HLA-DR and CD38. While lymphopenia was a constant finding in severely ill patients with acute SARS-CoV-2 infection [21], lymphopenia was not detected in our convalescent patient collective. Notably, thymic involution has been shown in the past to be associated with increased levels in the thymus of distinct cytokines, amongst them also interleukin (IL-6), which itself represents a promising biomarker for severely ill COVID-19 patients [60,61] and qualified in the recent past as a potent target for immune intervention in severely ill COVID-19 patients using Tocilizumab [62]. However, the relatively mild disease course of our COVID-19 convalescent patients did neither reveal reduced overall lymphocyte counts nor reduced thymic output 70 days after acute infection.

Apart from elevated numbers of memory T cells, we found elevated numbers of circulating plasmablasts, which are commonly referred to as a sign of recent antigen contact [63] and actue COVID-19 [22]. The elevated plasma cell precursor levels perfectly fit to the broad anti-SARS-CoV-2 antibody response in COVID-19 convalescents. In fact, all but one COVID-19 convalescent patient had specific antibody responses (108 tested; 107 positive) in the certified SARS-CoV-2 antibody test (Elecsys® Anti-SARS-CoV-2 assay, Roche). Interestingly, one COVID-19 convalescent patient was completely negative in the Roche test, although the patient was tested positive by rtPCR during acute disease. A closer look at this discrepant test result (PCR-test positive; NC-test negative) revealed that this patient underwent chemotherapeutic treatment for metastatic

This article is protected by copyright. All rights reserved

cancer. This patient presented not only with a negative NC-test value of 0.1 (cut-off level 1.0) but also had no specific anti-S or anti-RBD antibodies levels. The finding that individuals with a suppressed immune system may well be able to cope with COVID-19 and clear the virus without a clear sign of seroconversion is interesting because it indicates that virus clearance and disease resolution are eventually not only dependent on antibody responses.

Moreover, two patients clearly reacted in the NC-test (36.0 and 74.1, respectively), but no anti-S-protein or anti-RBD protein antibodies were detected. Together, these findings indicate that the spectrum and magnitude of antibody specificities in COVID-19 convalescent patients may considerably vary. In this context it will be interesting to perform a comprehensive analysis of the SARS-CoV-2-specific antibody response using a broad spectrum of virus-derived antigens and epitopes and testing of several isotypes and IgG subclasses by multiplex tests such as chips containing micro-arrayed components similar as developed for other viral infections [64,65].

The fact that more than 25% of the convalescent patients did not mount a relevant anti-RBD antibody response fits to our earlier finding that up to 50% of convalescent patients do not mount antibodies which can inhibit the docking of the virus via RBD to its receptor, ACE2 [9]. Also in this study we found that approximately 50-60% of COVID-19 convalescent patients have antibodies inhibiting the binding of RBD to ACE2 and hence may be considered to have neutralizing capacity, which confirmed the findings of our last study [9] (data not shown).

Whether antibodies binding to S-protein outside of the RBD have virus-neutralizing capacity or contribute to virus clearance by other mechanisms such as receptor-mediated clearance by immune cells remains to be investigated.

The percentages of pre-existing allergy/asthma in both groups were quite high (COVID-19 group: 34.8%; Control group: 43.9%), however, within the range reported for the general population in Austria [66]. Within the COVID-19 patient group, no significant associations between allergy and the self-reported severity of typical COVID-19 symptoms such as coughing (p=0.8413), shortness of breath (p=0.2906) or wheezing (p=0.0647) were evident.

This article is protected by copyright. All rights reserved

In summary, we provide compelling evidence for a considerable and protracted imprint of SARS-CoV-2 infection on the human immune system at different levels even after mild COVID-19 disease course. It is a limitation of our study that we have no data whether the COVID-19 patients besides SARS-CoV-2 had also other infections. However, their disease course was mild. Furthermore, the control subjects were from the same region and it is therefore likely that such other infections have affected both groups in a comparable manner. The observed differences between the COVID-19 and control group are therefore most likely caused by the SARS-CoV-2 infection. Specifically, SARS-CoV-2 infection seems to leave beneficial (i.e., activation of T cells, increased numbers of plasmablasts) and potentially harmful (i.e., reduction of neutrophils, reduction of Tregs) imprints in the cellular immune system in addition to the induction of specific antibody responses. Several aspects of our study are of potential clinical relevance: i) long fever duration was associated with increased T cell memory, i.e., central memory $CD4^+$ T help, which is in line with previous studies [67] and higher anti-S and anti-RBD but not NC antibody levels, potentially implicating that such COVID-19 convalescent individuals may have a better protection upon re-exposure to SARS-CoV-2; ii) however, patients unable to mount detectable anti-SARS-CoV-2 antibody levels may still be able to efficiently clear the virus and recover from COVID-19 diseases because we found one patient who had chemotherapy and, although this subject did not produce detectable SARS-CoV-2 antibodies recovered from COVID-19; iii) the reduced neutrophil numbers long after COVID-19 disease are stunning and warrant the search for possible underlying mechanisms (e.g., anti-neutrophil antibodies); iv) the dramatically low numbers of $CD4^+$ Treg cells requires further investigation to clarify if this is a potentially beneficial or harmful condition. On the one hand reduced $CD4^+$ Tregs may facilitate anti-SARS-CoV-2 immunity but eventually it could foster auto-reactivity; v) the long-term prevalence of HLA-DR- and CD38- expressing T cells may be a sign of robust SARS-CoV-2-specific immunity but may be also caused by persistence of antigen; vi) a more juvenile immune system, as determined by the numbers of RTE was associated with loss of sense of smell/taste as the main clinical symptom. It remains to be investigated if there is a causal relationship between these findings.

This article is protected by copyright. All rights reserved

Our study thus not only reports definitive evidence for a protracted immunological imprint of COVID-19 on human peripheral leukocyte populations but also raises several new aspects of COVID-19 which require further studies.

Accepted Article

This article is protected by copyright. All rights reserved

ACKNOWLEDGEMENTS

This study was supported by grants from the “Medizinisch-Wissenschaftlicher Fonds des Buergermeisters der Bundeshauptstadt Wien” (Medical-Scientific Fund of the Major of Vienna) COVID001 and COVID006; the Austrian Science Fund (FWF) grant DK-W1248, the Austrian Research Promotion Agency (FFG) COVID-19 emergency call grant 35721032, and Viravaxx, Vienna, Austria. The funders had no role in study design, data collection and analysis, decision to publish, or preparation of the manuscript. We thank Martina Trella for excellent technical assistance. Moreover, we wish to thank Dr. Gottfried F. Fischer for help with determining TREC and KREC numbers. We are grateful to Doris Werjant-Locmele and Anna Guentcheva for their help regarding recruitment and administration of study subjects. We are indebted to all individuals who participated in our study.

Accepted Article

This article is protected by copyright. All rights reserved

REFERENCES

1. Wang C, Horby PW, Hayden FG, Gao GF. A novel coronavirus outbreak of global health concern. *Lancet.* 2020;395(10223):470-473.
2. Zhang JJ, Dong X, Cao YY, et al. Clinical characteristics of 140 patients infected with SARS-CoV-2 in Wuhan, China. *Allergy.* 2020;75(7):1730-1741.
3. Zhu N, Zhang D, Wang W, et al. A Novel Coronavirus from Patients with Pneumonia in China, 2019. *N Engl J Med.* 2020;382(8):727-733.
4. Zhang YZ, Holmes EC. A Genomic Perspective on the Origin and Emergence of SARS-CoV-2. *Cell.* 2020;181(2):223-227.
5. Park M, Thwaites RS, Openshaw PJM. COVID-19: Lessons from SARS and MERS. *Eur J Immunol.* 2020;50(3):308-311.
6. World Health Organization. Coronavirus disease (COVID-19) outbreak. . 2020; https://www.who.int/emergencies/diseases/novel-coronavirus-2019.
7. Li W, Moore MJ, Vasilieva N, et al. Angiotensin-converting enzyme 2 is a functional receptor for the SARS coronavirus. *Nature.* 2003;426(6965):450-454.
8. Wan Y, Shang J, Graham R, Baric RS, Li F. Receptor Recognition by the Novel Coronavirus from Wuhan: an Analysis Based on Decade-Long Structural Studies of SARS Coronavirus. *J Virol.* 2020;94(7):doi: 10.1128/JVI.00127-00120.
9. Gattinger P, Borochova K, Dorofeeva Y, et al. Antibodies in serum of convalescent patients following mild COVID-19 do not always prevent virus-receptor binding. *Allergy.* 2020;doi: 10.1111/all.14523.
10. Ulrich H, Pillat MM. CD147 as a Target for COVID-19 Treatment: Suggested Effects of Azithromycin and Stem Cell Engagement. *Stem Cell Rev Rep.* 2020;16(3):434-440.
11. Jeffers SA, Hemmila EM, Holmes KV. Human coronavirus 229E can use CD209L (L-SIGN) to enter cells. *Adv Exp Med Biol.* 2006;581:265-269.
12. Jeffers SA, Tusell SM, Gillim-Ross L, et al. CD209L (L-SIGN) is a receptor for severe acute respiratory syndrome coronavirus. *Proc Natl Acad Sci U S A.* 2004;101(44):15748-15753.
13. Zhang R, Li Y, Zhang AL, Wang Y, Molina MJ. Identifying airborne transmission as the dominant route for the spread of COVID-19. *Proc Natl Acad Sci U S A.* 2020;117(26):14857-14863.

This article is protected by copyright. All rights reserved

14. Riggioni C, Comberiati P, Giovannini M, et al. A compendium answering 150 questions on COVID-19 and SARS-CoV-2. *Allergy.* 2020. doi:10.1111/all.14449
15. Huang C, Wang Y, Li X, et al. Clinical features of patients infected with 2019 novel coronavirus in Wuhan, China. *Lancet.* 2020;395(10223):497-506.
16. Azkur AK, Akdis M, Azkur D, et al. Immune response to SARS-CoV-2 and mechanisms of immunopathological changes in COVID-19. *Allergy.* 2020;75(7):1564-1581.
17. Wang D, Yin Y, Hu C, et al. Clinical course and outcome of 107 patients infected with the novel coronavirus, SARS-CoV-2, discharged from two hospitals in Wuhan, China. *Crit Care.* 2020;24(1):188.
18. Zhang JJ, Cao YY, Dong X, et al. Distinct characteristics of COVID-19 patients with initial rRT-PCR-positive and rRT-PCR-negative results for SARS-CoV-2. *Allergy.* 2020;75(7):1809-1812.
19. Wang F, Yao Y, Hou H, et al. Delayed virus-specific antibody responses associate with COVID-19 mortality. *Allergy.* 2020; doi: 10.1111/all.14546
20. Deng Z, Zhang M, Zhu T, et al. Dynamic changes in peripheral blood lymphocyte subsets in adult patients with COVID-19. *Int J Infect Dis.* 2020;98:353-358.
21. Jesenak M, Brndiarova M, Urbancikova I, et al. Immune Parameters and COVID-19 Infection - Associations With Clinical Severity and Disease Prognosis. *Front Cell Infect Microbiol.* 2020;10:364.
22. Kuri-Cervantes L, Pampena MB, Meng W, et al. Comprehensive mapping of immune perturbations associated with severe COVID-19. *Sci Immunol.* 2020;5(49).
23. Odak I, Barros-Martins J, Bosnjak B, et al. Reappearance of effector T cells is associated with recovery from COVID-19. *EBioMedicine.* 2020;57:102885.
24. Song J-W, Zhang C, Fan X, et al. Immunological and inflammatory profiles in mild and severe cases of COVID-19. *Nat Commun.* 2020;11(1):3410.
25. Xu B, Fan C-Y, Wang A-L, et al. Suppressed T cell-mediated immunity in patients with COVID-19: A clinical retrospective study in Wuhan, China. *The Journal of infection.* 2020;81(1):e51-e60.
26. Yip CYC, Yap ES, De Mel S, et al. Temporal changes in immune blood cell parameters in COVID-19 infection and recovery from severe infection. *Br J Haematol.* 2020;190(1):33-36.

Accepted Article

This article is protected by copyright. All rights reserved

27. Yuan X, Huang W, Ye B, et al. Changes of hematological and immunological parameters in COVID-19 patients. *Int J Hematol.* 2020;10.1007/s12185-020-02930-w.
28. Qin C, Zhou L, Hu Z, et al. Dysregulation of Immune Response in Patients With Coronavirus 2019 (COVID-19) in Wuhan, China. *Clin Infect Dis.* 2020;71(15):762-768.
29. Wang F, Nie J, Wang H, et al. Characteristics of Peripheral Lymphocyte Subset Alteration in COVID-19 Pneumonia. *J Infect Dis.* 2020;221(11):1762-1769.
30. Zhao J, Zhao J, Mangalam AK, et al. Airway Memory CD4(+) T Cells Mediate Protective Immunity against Emerging Respiratory Coronaviruses. *Immunity.* 2016;44(6):1379-1391.
31. Shah VK, Firmal P, Alam A, Ganguly D, Chattopadhyay S. Overview of Immune Response During SARS-CoV-2 Infection: Lessons From the Past. *Front Immunol.* 2020;11:1949.
32. Fan YY, Huang ZT, Li L, et al. Characterization of SARS-CoV-specific memory T cells from recovered individuals 4 years after infection. *Arch Virol.* 2009;154(7):1093-1099.
33. Sekine T, Perez-Potti A, Rivera-Ballesteros O, et al. Robust T cell immunity in convalescent individuals with asymptomatic or mild COVID-19. *Cell.* 2020;doi: 10.1016/j.cell.2020.08.017.
34. Perkmann T, Perkmann-Nagele N, Breyer MK, et al. Side by side comparison of three fully automated SARS-CoV-2 antibody assays with a focus on specificity. *Clin Chem.* 2020;doi: 10.1093/clinchem/hvaa198.
35. Cossarizza A, Chang HD, Radbruch A, et al. Guidelines for the use of flow cytometry and cell sorting in immunological studies (second edition). *Eur J Immunol.* 2019;49(10):1457-1973.
36. Segel GB, Halterman JS. Neutropenia in pediatric practice. *Pediatr Rev.* 2008;29(1):12-23;.
37. Ko HS, Fu SM, Winchester RJ, Yu DT, Kunkel HG. Ia determinants on stimulated human T lymphocytes. Occurrence on mitogen- and antigen-activated T cells. *J Exp Med.* 1979;150(2):246-255.

This article is protected by copyright. All rights reserved

38. Ho HN, Hultin LE, Mitsuyasu RT, et al. Circulating HIV-specific CD8+ cytotoxic T cells express CD38 and HLA-DR antigens. *J Immunol.* 1993;150(7):3070-3079.
39. Kestens L, Vanham G, Gigase P, et al. Expression of activation antigens, HLA-DR and CD38, on CD8 lymphocytes during HIV-1 infection. *AIDS.* 1992;6(8):793-797.
40. Appay V, van Lier RA, Sallusto F, Roederer M. Phenotype and function of human T lymphocyte subsets: consensus and issues. *Cytometry A.* 2008;73(11):975-983.
41. Boldt A, Borte S, Fricke S, et al. Eight-color immunophenotyping of T-, B-, and NK-cell subpopulations for characterization of chronic immunodeficiencies. *Cytometry B Clin Cytom.* 2014;86(3):191-206.
42. Cai Q, Huang D, Ou P, et al. COVID-19 in a designated infectious diseases hospital outside Hubei Province, China. *Allergy.* 2020;75(7):1742-1752.
43. Ferrario CM, Jessup J, Chappell MC, et al. Effect of angiotensin-converting enzyme inhibition and angiotensin II receptor blockers on cardiac angiotensin-converting enzyme 2. *Circulation.* 2005;111(20):2605-2610.
44. Schooley RT, Densen P, Harmon D, et al. Antineutrophil antibodies in infectious mononucleosis. *Am J Med.* 1984;76(1):85-90.
45. Havens WP, Jr., Marck RE. The leukocytic response of patients with experimentally induced infectious hepatitis. *Am J Med Sci.* 1946;212(2):129-138.
46. Thatte UM, Gangal PS, Kulkarni MR, Anklesaria PS, Kumta NB, Dahanukar SA. Polymorphonuclear and monocyte functions in measles. *J Trop Pediatr.* 1991;37(2):67-70.
47. Koumbourlis AC, Heldrich FJ. Varicella infection with profound neutropenia, multisystem involvement and no sequelae. *Pediatr Infect Dis J.* 1988;7(6):429-430.
48. Bartelloni PJ, Tesh RB. Clinical and serologic responses of volunteers infected with phlebotomus fever virus (Sicilian type). *Am J Trop Med Hyg.* 1976;25(3):456-462.
49. Hillenbrand FK. The blood picture in rubella; its place in diagnosis. *Lancet.* 1956;271(6933):66-68.
50. Viallard JF, Bloch-Michel C, Neau-Cransac M, et al. HLA-DR expression on lymphocyte subsets as a marker of disease activity in patients with systemic lupus erythematosus. *Clin Exp Immunol.* 2001;125(3):485-491.
51. Saez-Cirion A, Lacabaratz C, Lambotte O, et al. HIV controllers exhibit potent CD8 T cell capacity to suppress HIV infection ex vivo and peculiar cytotoxic T

This article is protected by copyright. All rights reserved

lymphocyte activation phenotype. *Proc Natl Acad Sci U S A.* 2007;104(16):6776-6781.
52. Mathew D, Giles JR, Baxter AE, et al. Deep immune profiling of COVID-19 patients reveals distinct immunotypes with therapeutic implications. *Science.* 2020;369(6508).
53. Holling TM, Schooten E, van Den Elsen PJ. Function and regulation of MHC class II molecules in T-lymphocytes: of mice and men. *Hum Immunol.* 2004;65(4):282-290.
54. Gerard A, Khan O, Beemiller P, et al. Secondary T cell-T cell synaptic interactions drive the differentiation of protective CD8+ T cells. *Nat Immunol.* 2013;14(4):356-363.
55. Ausiello CM, Urbani F, la Sala A, Funaro A, Malavasi F. CD38 ligation induces discrete cytokine mRNA expression in human cultured lymphocytes. *Eur J Immunol.* 1995;25(5):1477-1480.
56. Deaglio S, Morra M, Mallone R, et al. Human CD38 (ADP-ribosyl cyclase) is a counter-receptor of CD31, an Ig superfamily member. *J Immunol.* 1998;160(1):395-402.
57. Dianzani U, Funaro A, DiFranco D, et al. Interaction between endothelium and CD4+CD45RA+ lymphocytes. Role of the human CD38 molecule. *J Immunol.* 1994;153(3):952-959.
58. Ahmed R, Gray D. Immunological memory and protective immunity: understanding their relation. *Science.* 1996;272(5258):54-60.
59. Paul WE. *Fundamental Immunology.* Philadelphia: Lippincott Williams &Wilkins; 2013.
60. Chen X, Zhao B, Qu Y, et al. Detectable serum SARS-CoV-2 viral load (RNAaemia) is closely correlated with drastically elevated interleukin 6 (IL-6) level in critically ill COVID-19 patients. *Clin Infect Dis.* 2020;doi: 10.1093/cid/ciaa449.
61. Chakraborty C, Sharma AR, Bhattacharya M, Sharma G, Lee SS, Agoramoorthy G. COVID-19: Consider IL-6 receptor antagonist for the therapy of cytokine storm syndrome in SARS-CoV-2 infected patients. *J Med Virol.* 2020;doi: 10.1002/jmv.26078.
62. Xu X, Han M, Li T, et al. Effective treatment of severe COVID-19 patients with tocilizumab. *Proc Natl Acad Sci U S A.* 2020;117(20):10970-10975.

Accepted Article

This article is protected by copyright. All rights reserved

63. Mei HE, Yoshida T, Sime W, et al. Blood-borne human plasma cells in steady state are derived from mucosal immune responses. *Blood.* 2009;113(11):2461-2469.
64. Gallerano D, Wollmann E, Lupinek C, et al. HIV microarray for the mapping and characterization of HIV-specific antibody responses. *Lab Chip.* 2015;15(6):1574-1589.
65. Niespodziana K, Stenberg-Hammar K, Megremis S, et al. PreDicta chip-based high resolution diagnosis of rhinovirus-induced wheeze. *Nat Commun.* 2018;9(1):2382.
66. Stemeseder T, Klinglmayr E, Moser S, et al. Cross-sectional study on allergic sensitization of Austrian adolescents using molecule-based IgE profiling. *Allergy.* 2017;72(5):754-763.
67. Peng Y, Mentzer AJ, Liu G, et al. Broad and strong memory CD4(+) and CD8(+) T cells induced by SARS-CoV-2 in UK convalescent individuals following COVID-19. *Nat Immunol.* 2020.

Accepted Article

This article is protected by copyright. All rights reserved

TABLE AND FIGURE LEGENDS

TABLE 1. Demographics, clinical presentation and preexisting health conditions of COVID-19 convalescent patients and healthy control subjects.

TABLE 2. Varimax-rotated factor structure for reported clinical symptoms of COVID-19 patients.

FIGURE 1. Impact of primary SARS-CoV-2 infection on absolute counts of leukocyte subpopulations as determined 10 weeks after disease onset. Shown are absolute values of the indicated leukocyte populations in peripheral blood of healthy control subjects (HC) and COVID-19 convalescent patients (COVID-19). Bars show mean values, whiskers the standard deviation, and open circles the values of single individuals. Data show pooled results of daily stainings (whole blood, 6-9 individuals per day) of n=98 for HC, and n=109 for COVID-19 patients, except for panels determining HLA-DR expression where n=97 for HC. P-values were determined by Mann-Whitney U-test and are indicated.

FIGURE 2. Impact of primary SARS-CoV-2 infection on relative amounts of T cell subpopulations and TREC levels as determined 10 weeks after disease onset. Shown are the relative values of selected T cell subpopulations in PB of healthy control subjects (HC) and COVID-19 convalescent patients (COVID-19). Bars show mean values, whiskers the standard deviation, and open circles the values of single individuals. Data show pooled results of daily stainings (whole blood, 5-9 individuals per day) and TREC analyses of n=98 for HC, and n=109 for COVID-19 patients, except for panels determining CD25/Foxp3 n=97 for HC; and CD45RO/CCR7 n=95 for HC and n=105 for COVID-19. P-values were determined by Mann-Whitney U-test and are indicated. TREC, T cell receptor excision circles.

FIGURE 3. Impact of primary SARS-CoV-2 infection on relative amounts of B cell subpopulations and KREC levels as determined 10 weeks after disease onset. Shown are the relative values of the indicated B cell sub populations in PB of healthy control subjects (HC) and COVID-19 convalescent patients (COVID-19). Bars show mean

This article is protected by copyright. All rights reserved

Accepted Article

values, whiskers the standard deviation, and open circles the values of single individuals. Data show pooled results of daily stainings (whole blood, 5-9 individuals per day) and KREC analyses of n=78 for HC, and n=108 for COVID-19 patients, except for KREC analyses n=98 for HC and n=109 for COVID-19. P-values were determined by Mann-Whitney U-test and are indicated. KREC, kappa-deleting recombination excision circles.

FIGURE 4. Clinical symptoms of COVID-19 patients and their correlation with immune cellular and humoral immune parameters. **A,** Shown are the frequencies of symptoms observed in COVID-19 patients (n=109). **B to H,** Shown are the correlations of cellular (B to E) and humoral (F to H) immune parameters with typical COVID-19 symptoms (n=85 in B; n=109 in C; n=23 for no and n=84 for fever in D; n=109 for E, F and n=108 for G; n=37 for no and n=72 for loss of taste/smell in H). In B only patients presenting with fever are shown. Statistical significance was determined by Mann-Whitney U-test for categorical values and by Pearson's correlation for continuous values. Lines in B, C and F to H represent the trend. COI, cut-off index.

Accepted Article

This article is protected by copyright. All rights reserved

TABLE 1. Demographics, clinical presentation and preexisting health conditions of COVID-19 convalescent patients and healthy control subjects.

Characteristics no. (%)	**COVID-19 convalescent patients N=109**	**Healthy control subjects N=98**
Female sex	48 (44.0)	54 (55.1)
Age Median (Range)	52 (16-78)	51 (14-77)
(Mean±SD)	50.1±14.1	50.1±14.2
Height in cm (Mean±SD)	175.6±8.9	172.2±8.9
Weight in kg (Mean±SD)	78.1±16.9	73.7±16.4
Positive PCR COVID-19 test	92 (84.4)	0 (0)
Positive antibody test (Roche)	103 (94.5)	0 (0)
Sneeze	**27 (24.8)**	**0 (0)**
Mild	21 (19.3)	0 (0)
Moderate	5 (4.6)	0 (0)
Strong	1 (0.9)	0 (0)
Runny nose	**32 (29.4)**	**0 (0)**
Mild	21 (19.3)	0 (0)
Moderate	9 (8.3)	0 (0)
Strong	2 (1.8)	0 (0)
Nasal congestion	**47 (43.1)**	**0 (0)**
Mild	29(26.6)	0 (0)
Moderate	11 (10.1)	0 (0)
Strong	7 (6.4)	0 (0)
Conjunctivitis	**13 (11.9)**	0 (0)
Mild	9 (8.3)	0 (0)
Moderate	3 (2.8)	0 (0)
Strong	1 (0.9)	0 (0)

Accepted Article

This article is protected by copyright. All rights reserved

Arthralgia	**55 (50.5)**	**0 (0)**
Mild	18 (16.5)	0 (0)
Moderate	16 (14.7)	0 (0)
Strong	21 (19.3)	0 (0)
Myalgia	**56 (51.4)**	0 (0)
Mild	18 (16.5)	0 (0)
Moderate	12 (11.0)	0 (0)
Strong	26 (23.9)	0 (0)
Nausea	**22 (20.2)**	**0 (0)**
Mild	14 (12.8)	0 (0)
Moderate	5 (4.6)	0 (0)
Strong	3 (2.8)	0 (0)
Headache	**72 (66.1)**	**0 (0)**
Mild	19 (17.4)	0 (0)
Moderate	22 (20.2)	0 (0)
Strong	31 (28.4)	0 (0)
Chills or rigor	**54 (49.5)**	0 (0)
Mild	23 (21.1)	0 (0)
Moderate	18 (16.5)	0 (0)
Strong	13 (11.9)	0 (0)
Fever	**84 (77.1)**	**0 (0)**
Max. temperature in °C Median (Range) Mean±SD	38.5 (37.1-42.0) 38.5±0.8	n.a.
<37.5°C	2 (1.8)	n.a.
37.5-38.0°C	23 (21.1)	n.a.
38.1-39.0°C	43 (39.4)	n.a.
>39.0°C	17 (15.6)	n.a.
Fever duration in days (Mean±SD)	**4.3±4.8**	n.a.

Accepted Article

This article is protected by copyright. All rights reserved

Diarrhea	**30 (27.5)**	**0 (0)**
Mild	19 (17.4)	0 (0)
Moderate	10 (9.2)	0 (0)
Strong	1 (0.9)	0 (0)
Loss of taste/smell	**72 (66.1)**	**0 (0)**
Mild	19 (17.4)	0 (0)
Moderate	15 (13.8)	0 (0)
Strong	38 (34.9)	0 (0)
Fatigue	**92 (84.4)**	**0 (0)**
Mild	28 (25.7)	0 (0)
Moderate	19 (17.4)	0 (0)
Strong	45 (41.3)	0 (0)
Vomiting	**7 (6.4)**	**0 (0)**
Mild	7 (6.4)	0 (0)
Moderate	0 (0)	0 (0)
Strong	0 (0)	0 (0)
Other GI problems	**7 (6.4)**	**0 (0)**
Sore throat	**42 (38.5)**	**0 (0)**
Mild	27 (24.8)	0 (0)
Moderate	13 (11.9)	0 (0)
Strong	2 (1.8)	0 (0)
Cough	**76 (69.7)**	**0 (0)**
Mild	35 (32.1)	0 (0)
Moderate	20 (18.3)	0 (0)
Strong	21 (19.3)	0 (0)
Wheezing	**26 (23.9)**	0 (0)
Mild	11 (10.1)	0 (0)
Moderate	11 (10.1)	0 (0)

Accepted Article

This article is protected by copyright. All rights reserved

Strong	4 (3.7)	0 (0)
Shortness of breath	**46 (42.2)**	**0 (0)**
Mild	19 (17.4)	0 (0)
Moderate	18 (16.5)	0 (0)
Strong	9 (8.3)	0 (0)
Pneumonia	**5 (4.6)**	0 (0)
Mild	4 (3.7)	0 (0)
Moderate	**1 (0.9)**	**0 (0)**
Strong	0 (0)	0 (0)
Days of illness (Symptoms)	**15.5±13.5**	**n.a.**
Symptom-free days to venipuncture	**55.3±18.0**	**>70**
Days between start of disease and venipuncture	**71.2±16.5**	**n.a.**
Hospitalized	**8 (7.3)**	0 (0)
Days of hospitalization	**5.9±5.8**	0 (0)
ICU or IMCU admission	0 (0)	0 (0)
Days spent in ICU	0 (0)	0 (0)
O2 therapy required	3 (2.75)	0 (0)
Days of O2 therapy	3.0±3.0	0 (0)
Invasive ventilation	0 (0)	0 (0)
Days of invasive ventilation	0 (0)	0 (0)
Asymptomatic	**3 (2.8)**	**98 (100)**
Preexisting health conditions	**71 (65.1)**	**64 (65.3)**
Cardiovascular diseases	22 (20.2)	19 (19.4)
Chronic lung diseases	15 (13.8)	11 (11.2)
Allergy/Asthma	38 (34.8)	43 (43.9)
Diabetes mellitus	3 (2.8)	4 (4.1)
Hematopoietic diseases	3 (2.8)	0 (0)

Accepted Article

This article is protected by copyright. All rights reserved

Immunosuppressive conditions	7 (6.4)	2 (2.0)
Liver diseases	2 (1.8)	3 (3.1)
Metabolic diseases	21 (19.3)	17 (17.3)
Neurological disorders	9 (8.3)	8 (8.1)
Renal diseases	4 (3.7)	3 (3.1)
Other medical problems	21 (19.3)	16 (16.3)
Pregnancy	0 (0)	0 (0)
Smoking	7 (6.4)	19 (19.4)
Regular alcohol consumption	41 (37.6)	36 (36.7)
Regular medications	**49 (45.0)**	**48 (49.0)**

Accepted Article

This article is protected by copyright. All rights reserved

TABLE 2. Varimax-rotated factor structure for reported clinical symptoms explainins a large proportion of the heterogeneity of clinical symptoms in COVID-19 patients.

	Factors						
Symptom Category	**F1**	**F2**	**F3**	**F4**	**F5**	**F6**	**F7**
Fever	0.758		0.183				-0.160
Chills or rigor	0.739		0.116		0.107		0.184
Fatigue	0.694	0.230	0.241			0.194	0.263
Cough	0.558			0.177	0.471	-0.112	0.258
Running nose		0.770			-0.102		
Nasal congestion		0.731		0.208		0.157	0.219
Sore throat	0.165	0.626	0.218	-0.125	0.394	0.113	
Sneeze	0.347	0.518	-0.244	0.135		-0.233	-0.172
Arthralgia			0.888	0.123			
Myalgia	0.242		0.845	0.119			
Conjunctivitis		0.146		0.759			0.273
Other GI problems			0.160	0.724			0.113
Pneumonia				-0.194	0.808	-0.143	
Shortness of breath	0.407			0.376	0.576	0.110	
Wheezing	0.317			0.472	0.525	0.387	-0.152
Vomiting		-0.145			-0.128	0.700	
Nausea	0.131	0.218	0.248	0.423	0.187	0.496	-0.168
Headache	0.225	0.297	0.393	-0.148		0.487	0.228
Diarrhea		0.446		0.246	0.108	0.475	0.217
Other symptoms				0.228		-0.115	0,772
Loss of taste/smell	0.155	0.223				0.312	0.663
Percent variance	22.7	10.7	8.8	7.0	6.1	5.3	4.8

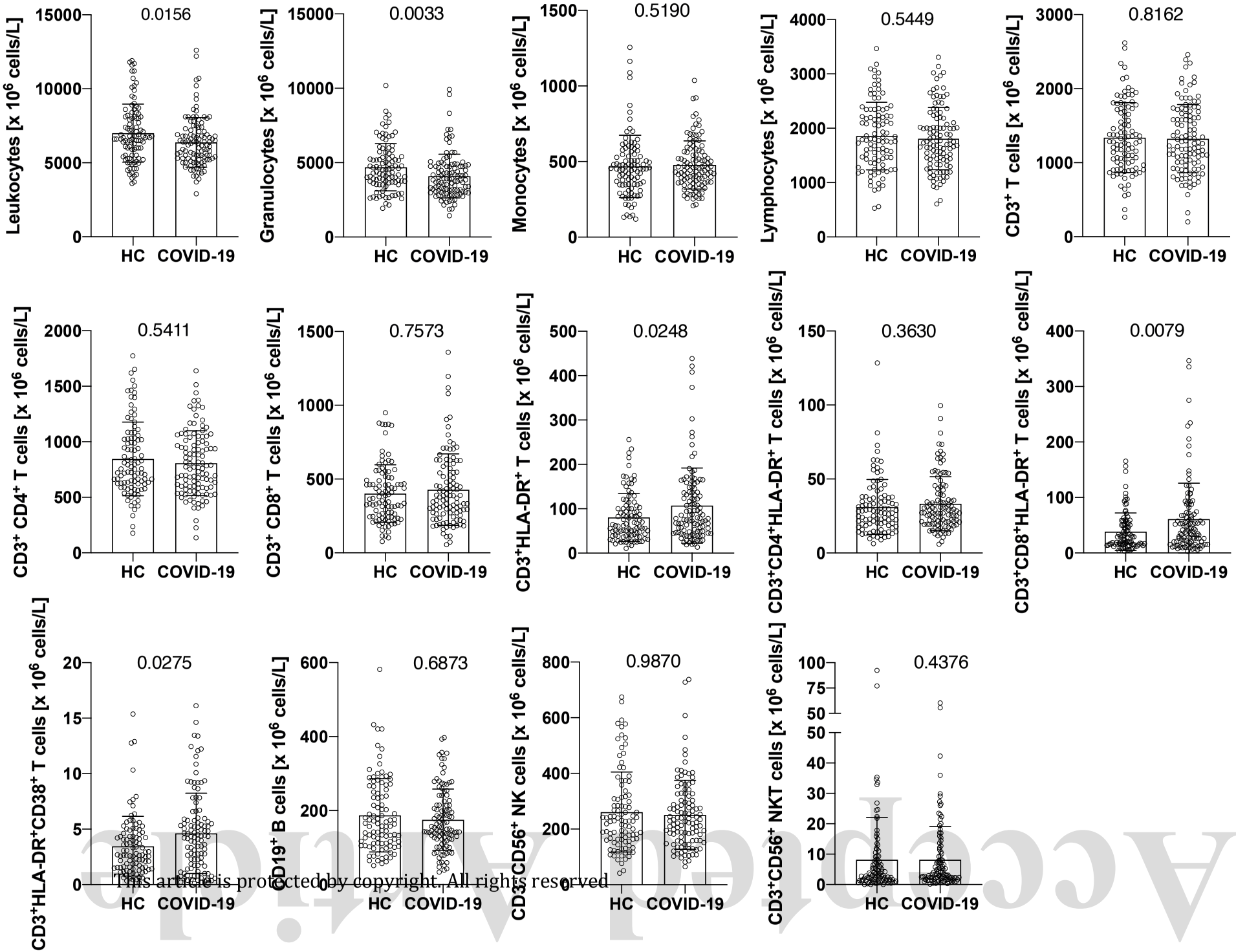
This article is protected by copyright. All rights reserved

The total amount of variance explained by the seven factors (F1-F7) defined by certain symptoms (factor 1: fever, chills, rigor, fatigue, cough; factor 2: running nose, nasal congestion, sore throat, sneeze; factor 3: arthralgia, myalgia; factor 4: conjunctivitis, other GI problems; factor 5: pneumonia, shortness of breath, wheezing; factor 6: vomiting, nausea, headache, diarrhea; factor 7: other symptoms, loss of taste, smell) adds up to 65.4%. The Kaiser-Meyer-Olkin criterion of 0.728 shows a middling value and the Bartlett-Test of sphericity is significant ($p<0.000$). Varimax-rotated factor loadings for the indicated groups of clinical symptoms. Loadings lower than 0.1 are omitted from the table. Gray background indicates grouped symptom (termed F1 to F7) displaying highest factor loadings.

Accepted Article

This article is protected by copyright. All rights reserved

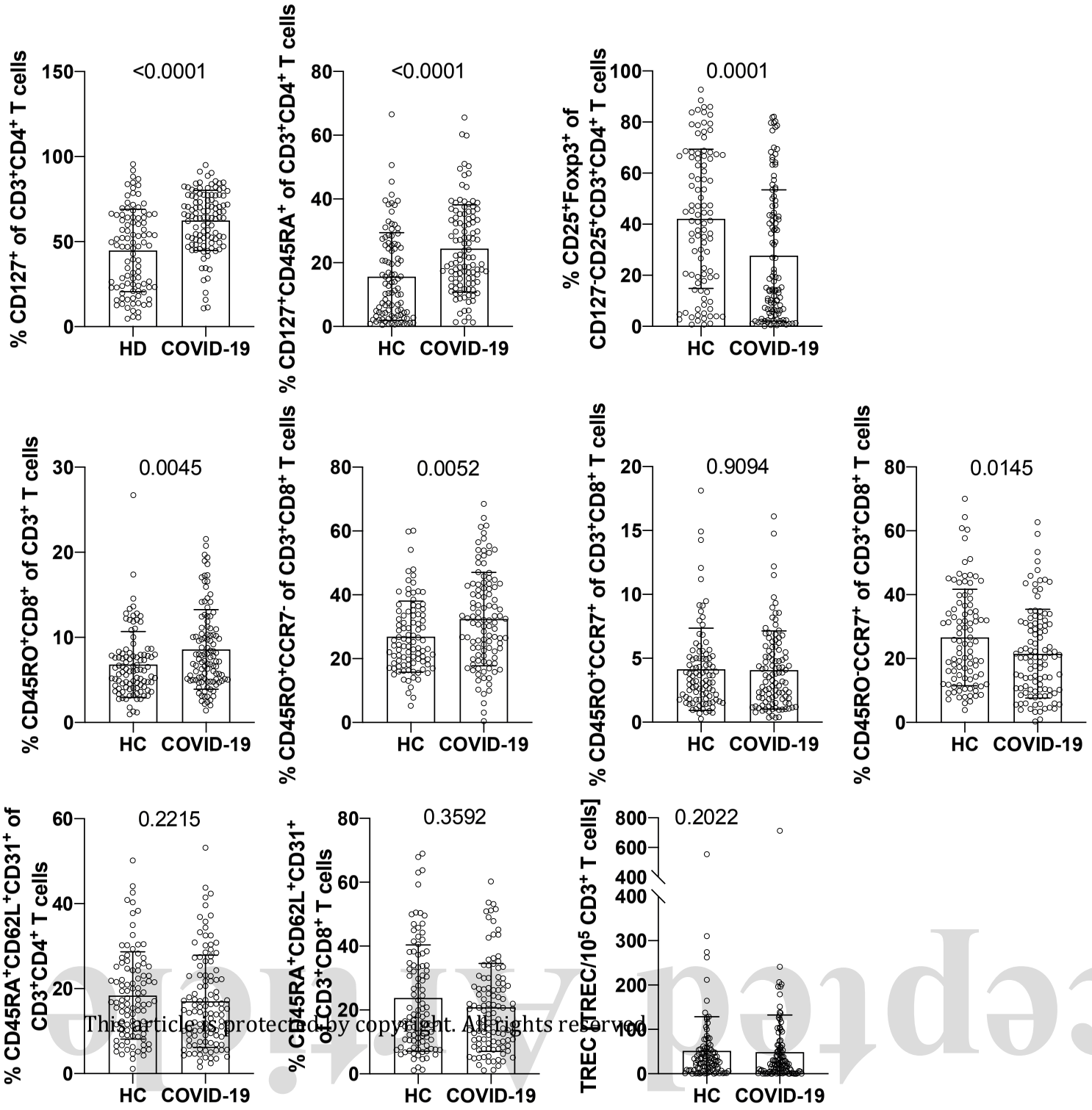
FIGURE 1



This article is protected by copyright. All rights reserved

Accepted Article

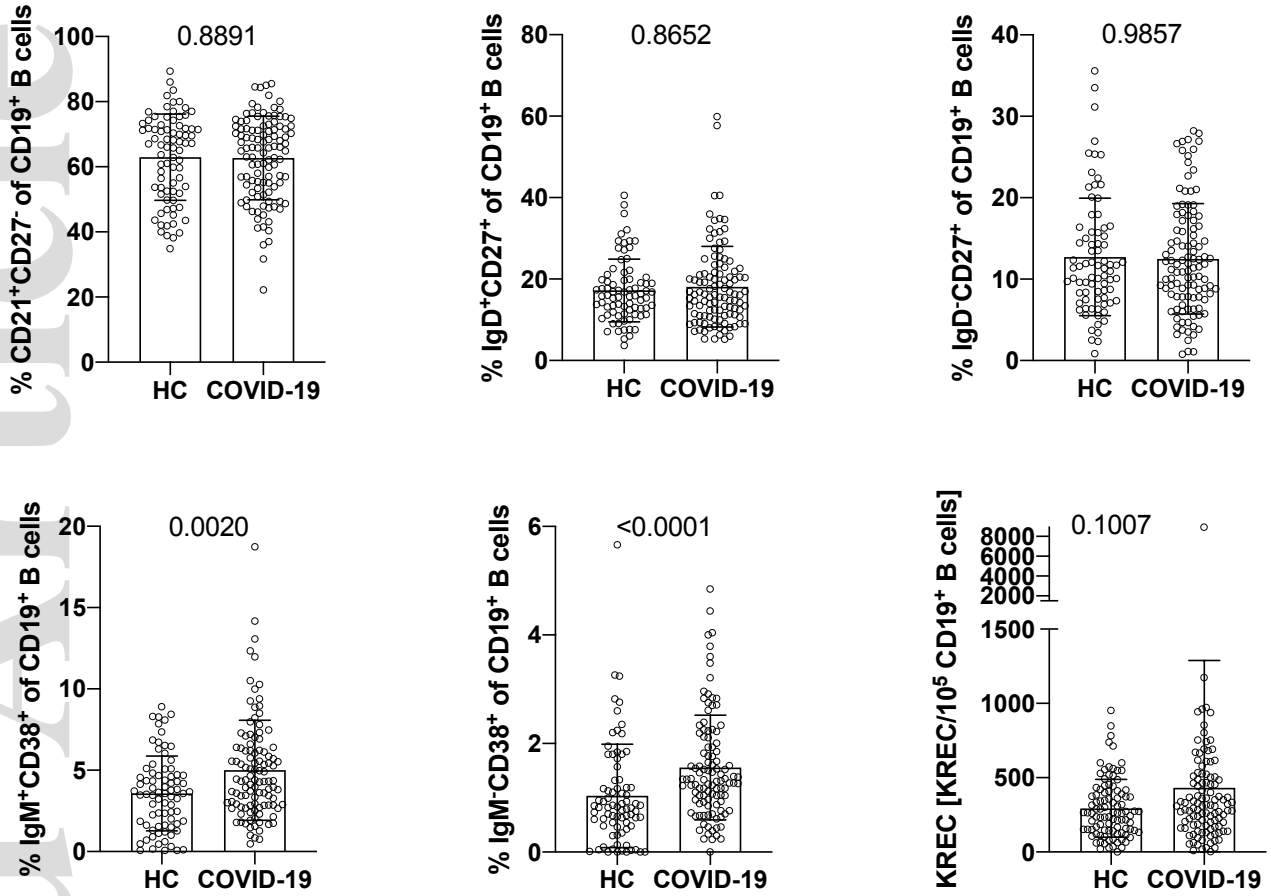
FIGURE 2



This article is protected by copyright. All rights reserved.

Accepted Article

FIGURE 3

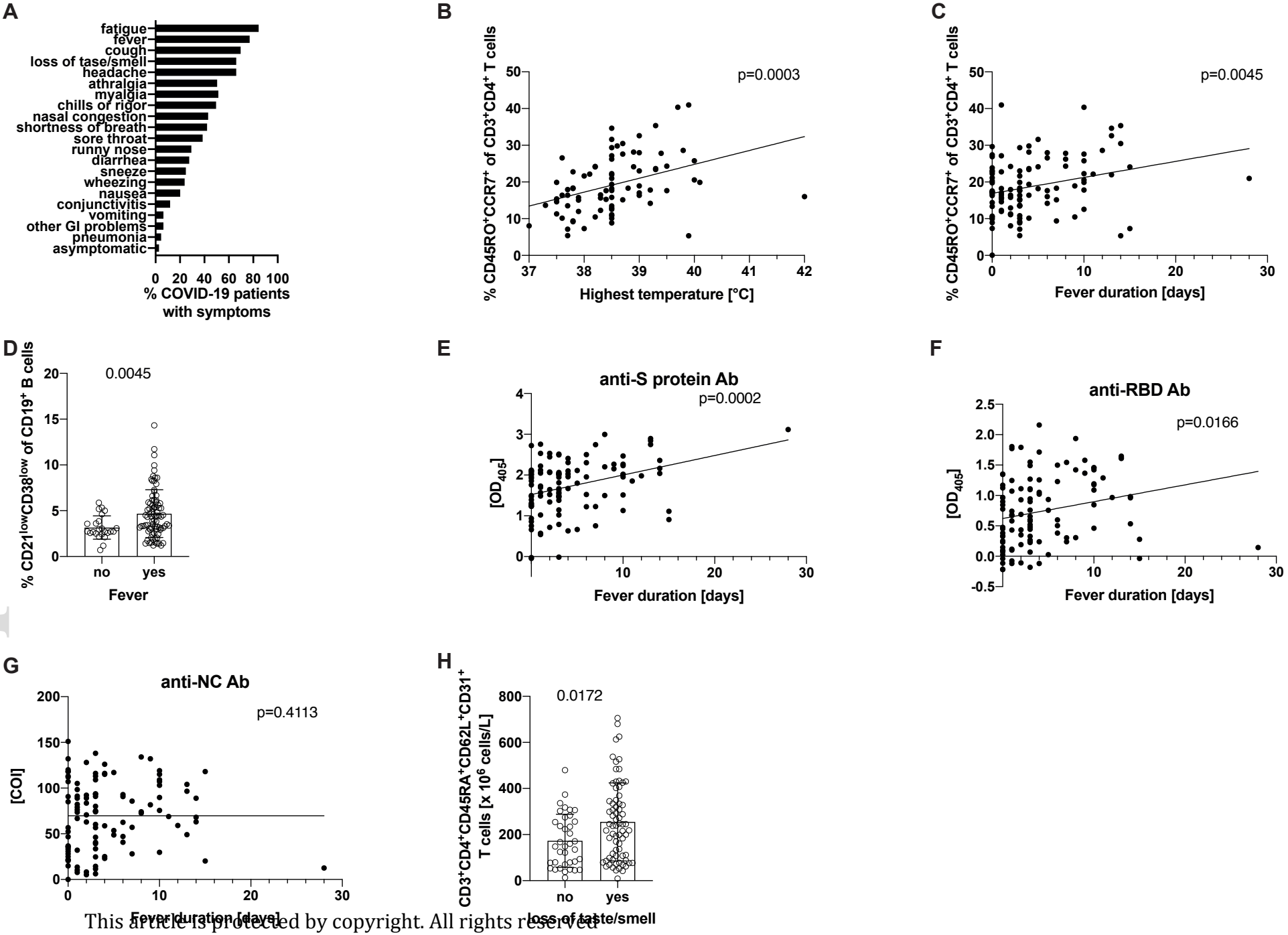


Accepted Article

This article is protected by copyright. All rights reserved

Accepted Article

FIGURE 4



This article is protected by copyright. All rights reserved

FIGURE S1

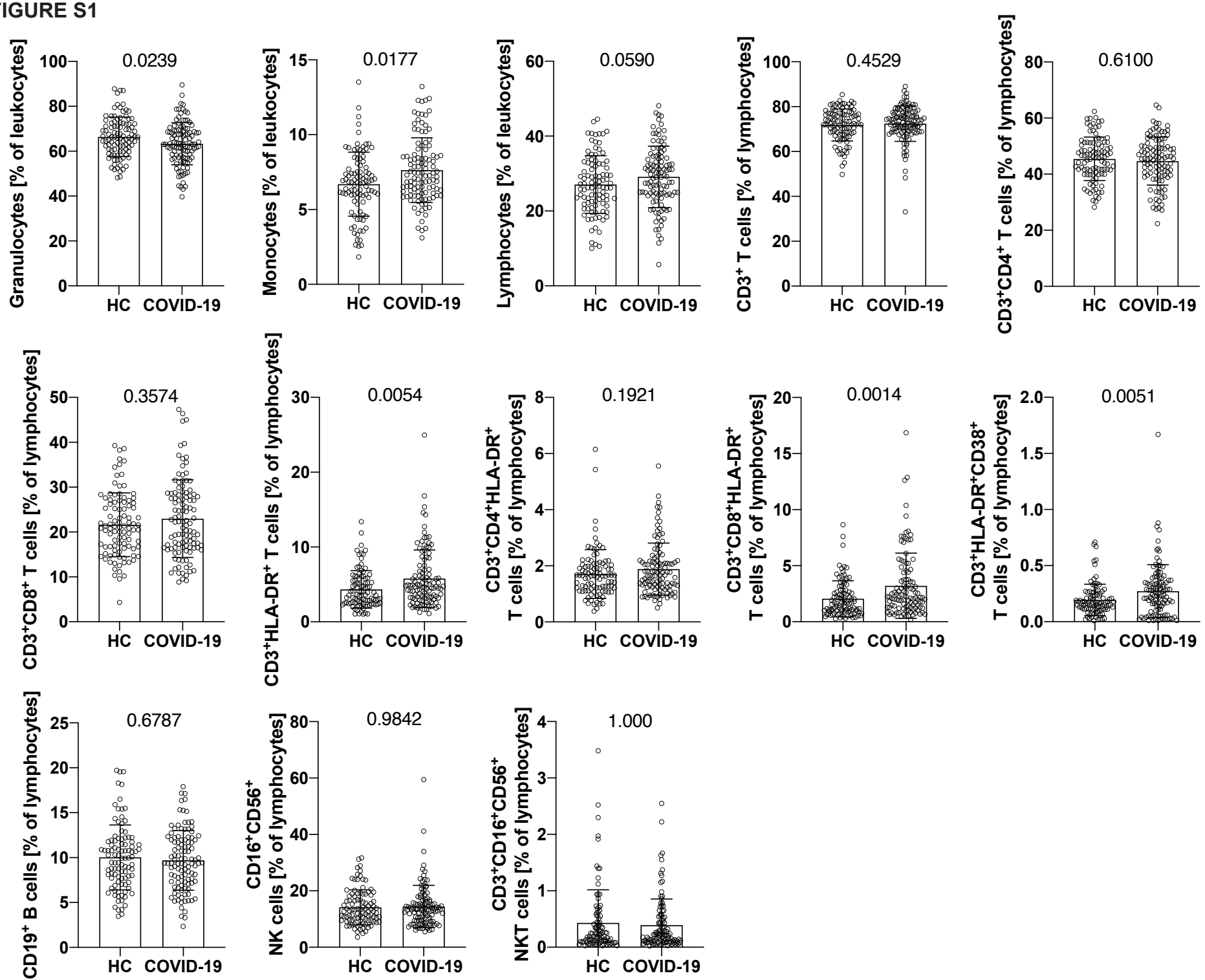

Granulocytes [% of leukocytes]
0.0239
Monocytes [% of leukocytes]
0.0177
Lymphocytes [% of leukocytes]
0.0590
CD3+ T cells [% of lymphocytes]
0.4529
CD3+CD4+ T cells [% of lymphocytes]
0.6100
CD3+CD8+ T cells [% of lymphocytes]
0.3574
CD3+HLA-DR+ T cells [% of lymphocytes]
0.0054
CD3+CD4+HLA-DR+ T cells [% of lymphocytes]
0.1921
CD3+CD8+HLA-DR+ T cells [% of lymphocytes]
0.0014
CD3+HLA-DR+CD38+ T cells [% of lymphocytes]
0.0051
CD19+ B cells [% of lymphocytes]
0.6787
CD16+CD56+ NK cells [% of lymphocytes]
0.9842
CD3+CD16+CD56+ NKT cells [% of lymphocytes]
1.000
HC
COVID-19

FIGURE S2

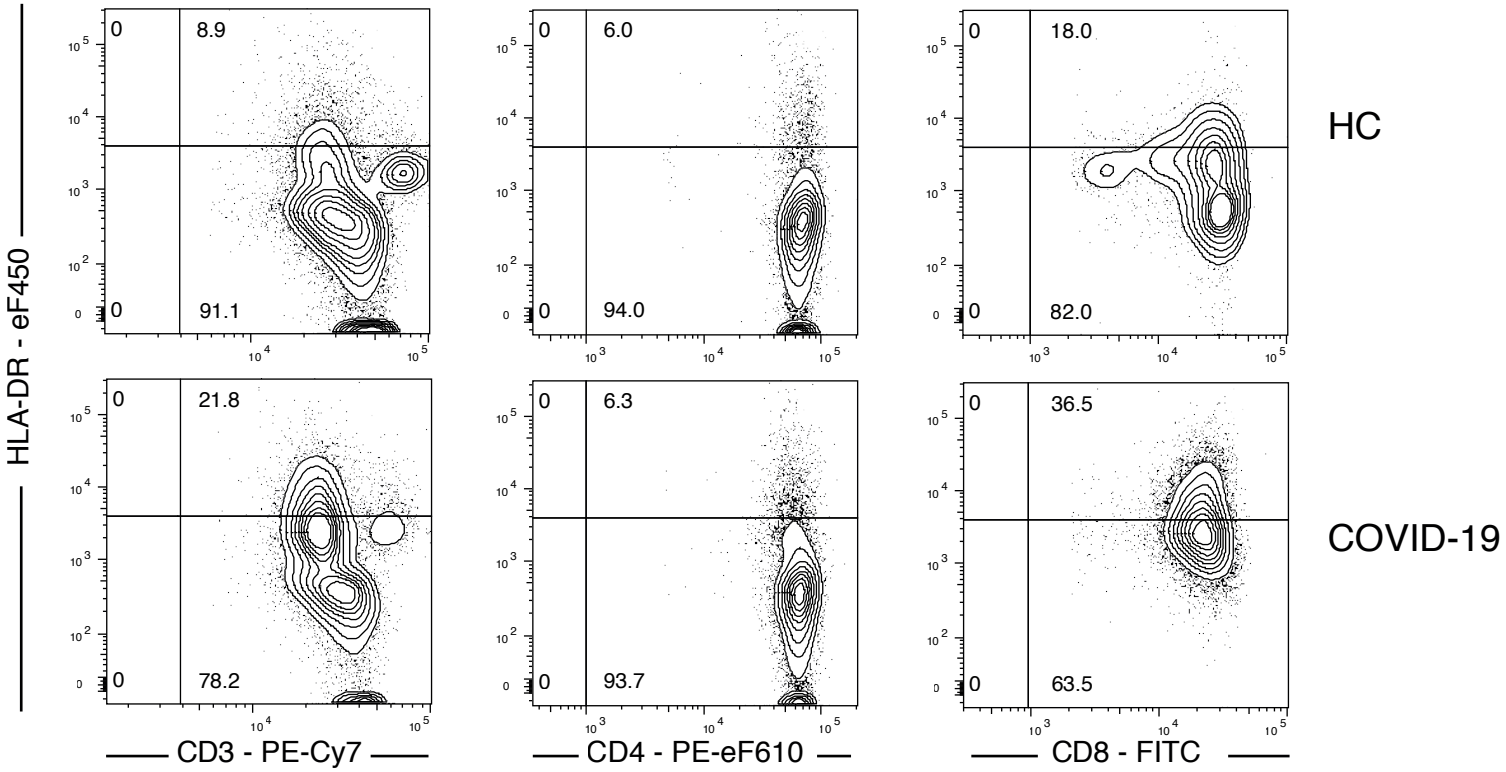

HLA-DR - eF450
0
8.9
91.1
6.0
94.0
18.0
82.0
HC
21.8
78.2
6.3
93.7
36.5
63.5
COVID-19
CD3 - PE-Cy7
CD4 - PE-eF610
CD8 - FITC

FIGURE S3

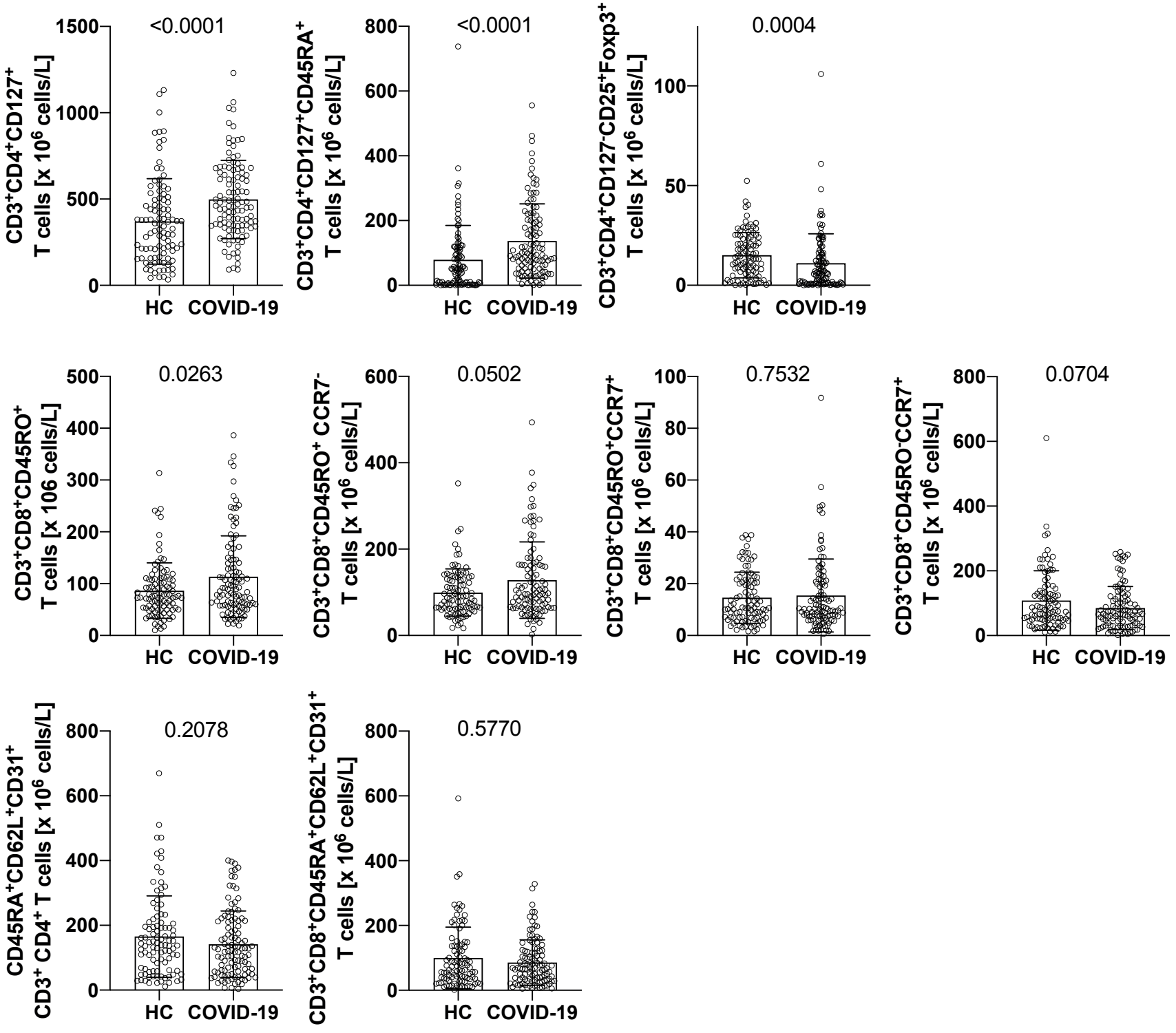
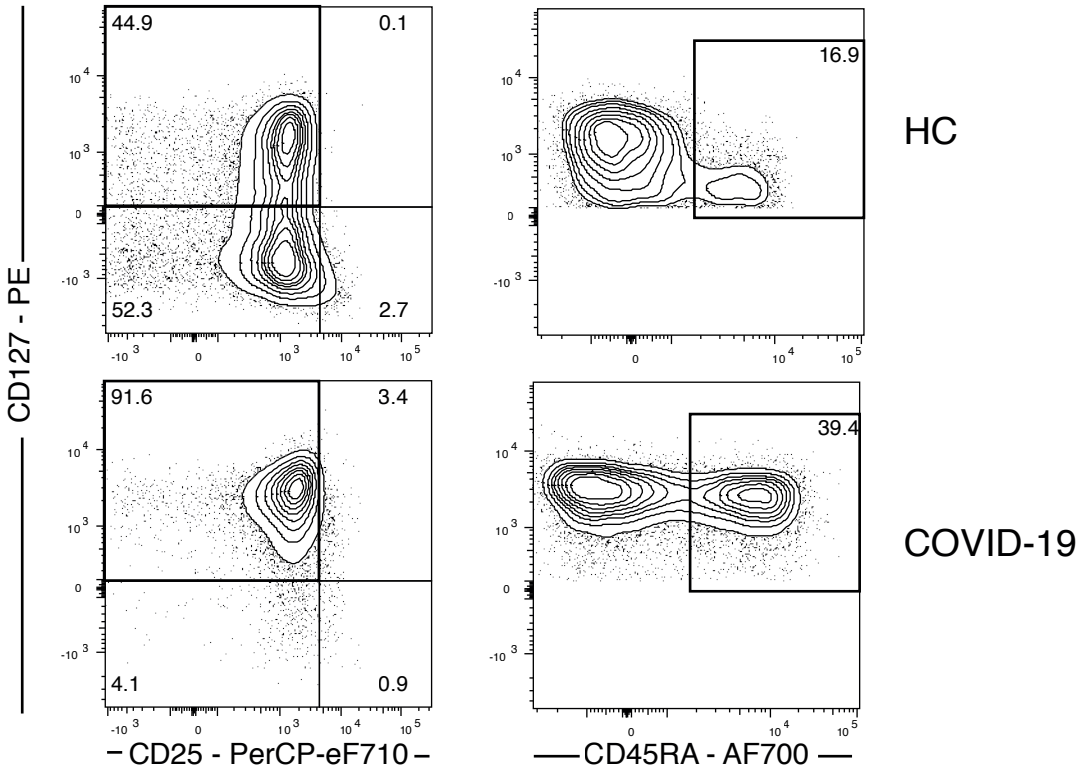

CD3+CD4+CD127+ T cells [x 10^6 cells/L]
<0.0001
HC
COVID-19
CD3+CD4+CD127+CD45RA+ T cells [x 10^6 cells/L]
<0.0001
CD3+CD4+CD127-CD25+Foxp3+ T cells [x 10^6 cells/L]
0.0004
CD3+CD8+CD45RO+ T cells [x 106 cells/L]
0.0263
CD3+CD8+CD45RO+ CCR7- T cells [x 10^6 cells/L]
0.0502
CD3+CD8+CD45RO+CCR7+ T cells [x 10^6 cells/L]
0.7532
CD3+CD8+CD45RO-CCR7+ T cells [x 10^6 cells/L]
0.0704
CD45RA+CD62L+CD31+ CD3+ CD4+ T cells [x 10^6 cells/L]
0.2078
CD3+CD8+CD45RA+CD62L+CD31+ T cells [x 10^6 cells/L]
0.5770

FIGURE S4


44.9
0.1
52.3
2.7
16.9
91.6
3.4
4.1
0.9
39.4
CD127 - PE
CD25 - PerCP-eF710
CD45RA - AF700
HC
COVID-19

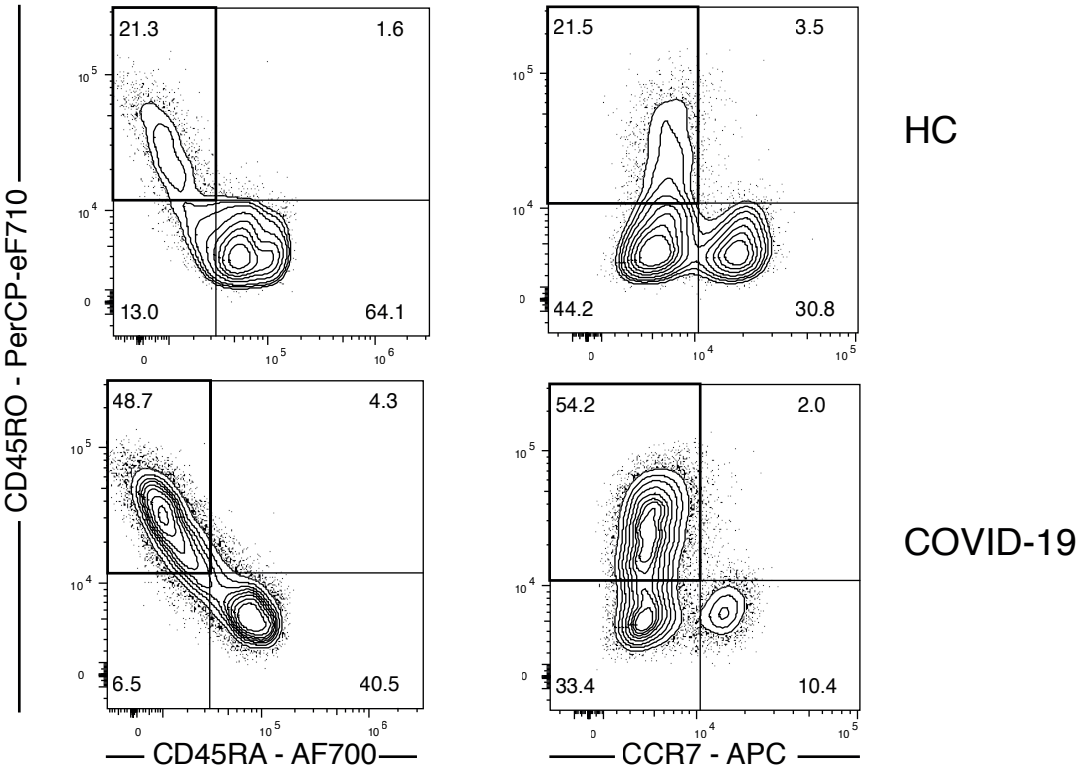

21.3
1.6
13.0
64.1
21.5
3.5
44.2
30.8
48.7
4.3
6.5
40.5
54.2
2.0
33.4
10.4
CD45RO - PerCP-eF710
CD45RA - AF700
CCR7 - APC
HC
COVID-19

FIGURE S5

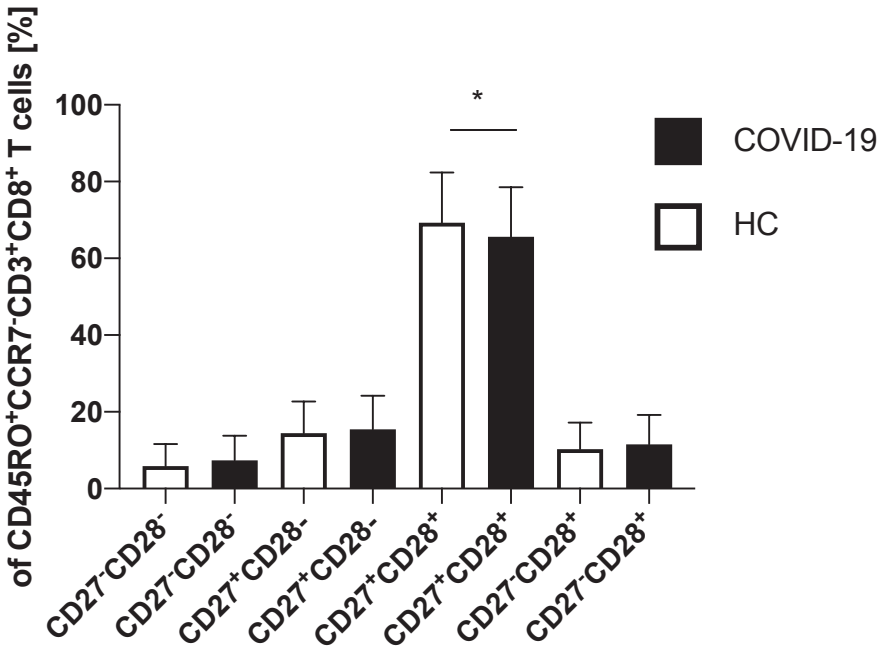

of CD45RO+CCR7-CD3+CD8+ T cells [%]
100
80
60
40
20
0
*
COVID-19
HC
CD27-CD28-
CD27-CD28-
CD27+CD28-
CD27+CD28-
CD27+CD28+
CD27+CD28+
CD27-CD28+
CD27-CD28+

FIGURE S6

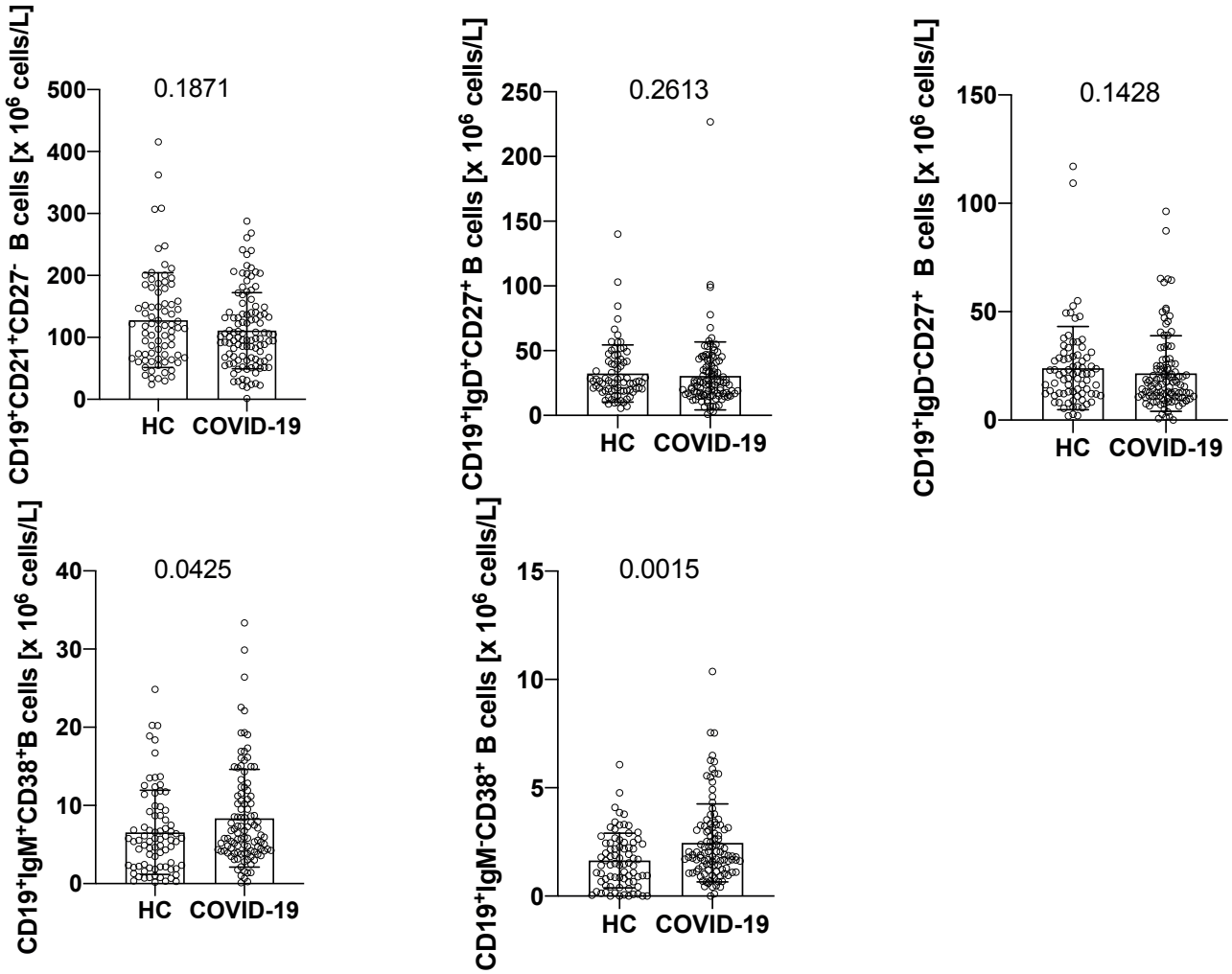

CD19+CD21+CD27- B cells [x 10^6 cells/L]
0.1871
HC
COVID-19
CD19+IgD+CD27+ B cells [x 10^6 cells/L]
0.2613
CD19+IgD-CD27+ B cells [x 10^6 cells/L]
0.1428
CD19+IgM+CD38+B cells [x 10^6 cells/L]
0.0425
CD19+IgM-CD38+ B cells [x 10^6 cells/L]
0.0015

FIGURE S7

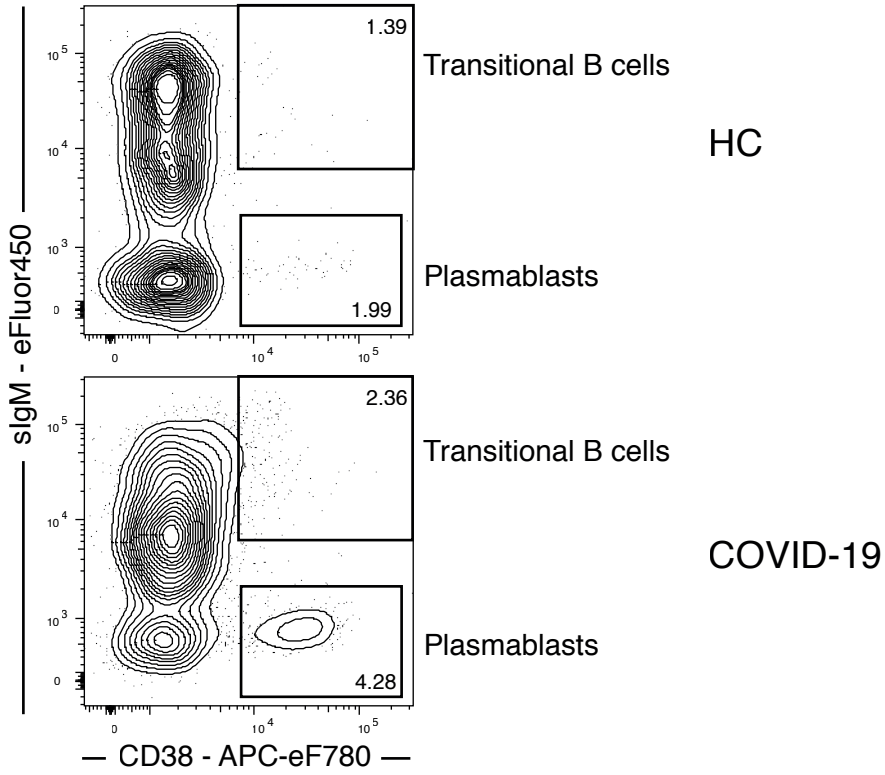
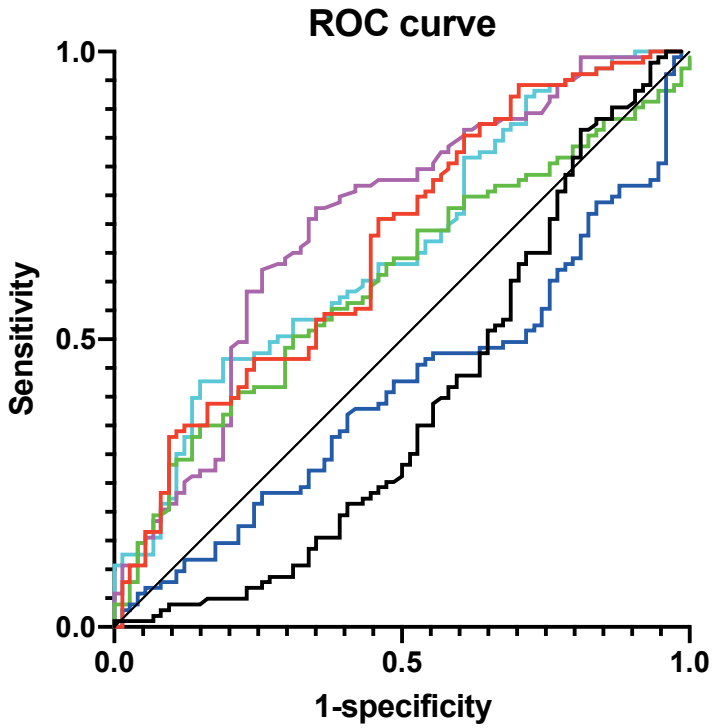

1.39
Transitional B cells
HC
Plasmablasts
1.99
2.36
Transitional B cells
COVID-19
Plasmablasts
4.28
sIgM - eFluor450
CD38 - APC-eF780

FIGURE S8



- %$CD3^+CD8^+CD27^+CD28^-CCR7^-CD45RA^{-/+}$ AE3 cells of $CD3^+CD8^+$ T cells
- %$CD3^+CD4^+CD127^+CD45RA^+$ of $CD3^+CD4^+$ T cells
- %$CD3^+CD4^+CD127^-CD25^+Foxp3^+CD45RA^+$ of $CD3^+CD4^+CD127^-CD25^+$T cells
- %$CD3^+CD8^+CD45RO^+CCR7^-$ of $CD3^+CD8^+$ T cells
- %$CD19^+IgM^-CD38^+$ plasmablasts of $CD19^+$ B cells
- %$CD19^+IgM^+CD38^+$ transitional B cells of $CD19^+$ B cells

Appendix S1

Online Repository

Bernhard Kratzer[1], Doris Trapin[1], Paul Ettel[1], Ulrike Körmoczi[1], Arno Rottal[1], Friedrich Tuppy[1], Melanie Feichter[1], Pia Gattinger[2], Kristina Borochova[2], Yulia Dorofeeva[2], Inna Tulaeva[2, 3], Milena Weber[2], Katharina Grabmeier-Pfistershammer[1], Peter Tauber[1], Marika Gerdov[4], Bernhard Mühl[5], Thomas Perkmann[4], Ingrid Fae[6], Sabine Wenda[6], Harald Führer[7], Rainer Henning[8], Rudolf Valenta[2, 3, 9, 10, *] and Winfried F. Pickl[1, *]

[1]Institute of Immunology, Center for Pathophysiology, Infectiology and Immunology, Medical University of Vienna, Vienna, Austria.
[2]Institute of Pathophysiology and Allergy Research, Center for Pathophysiology, Infectiology and Immunology, Medical University of Vienna, Vienna, Austria.
[3]Laboratory for Immunopathology, Department of Clinical Immunology and Allergology, I. M. Sechenov First Moscow State Medical University (Sechenov University), Moscow, Russia.
[4]Department of Laboratory Medicine, Medical University of Vienna, Vienna, Austria.
[5]Labors.at, Vienna, Austria.
[6] Department for Blood Group Serology and Transfusion Medicine, Medical University of Vienna, Vienna, Austria.
[7]Statistical Consultants, Vienna, Austria.
[8]Viravaxx, Vienna, Austria.
[9]NRC Institute of Immunology FMBA of Russia, Moscow, Russia.
[10]Karl Landsteiner University of Health Sciences, Krems, Austria.

***) Corresponding authors:**
Winfried F. Pickl, MD
Institute of Immunology, Center for Pathophysiology, Infectiology and Immunology, Medical University of Vienna, Lazarettgasse 19, 1090 Vienna, Austria.
Phone: (+431) 40160 33245.
Fax: (+431) 40160 933245.
Email: winfried.pickl@meduniwien.ac.at.
ORCID ID: orcid.org/0000-0003-0430-4952
&
Rudolf Valenta
Department of Pathophysiology and Allergy Research

Medical University of Vienna
Waehringer Guertel 18-20
A-1090 Vienna, Austria
Tel: (+431) 40400 51080
Fax: (+431) 40400 51300
E-mail: rudolf.valenta@meduniwien.ac.at
ORCID ID: 0000-0001-5944-3365

SUPPLEMENTAL MATERIALS AND METHODS

Immunophenotyping by multiparametric flow cytometry

Briefly, EDTA-anticoagulated blood was washed three times with PBS and 50 to 100 µl were incubated with optimal concentrations of the antibodies listed in **Table S1**. Samples were incubated with the respective antibody mix for 15 minutes, followed by the addition of 100 µl Nordic lyse (Nordic MUbio, Susteren, The Netherlands) and incubated for 10 minutes. Subsequently, 4.5 ml of double distilled H_20 was added to each sample, incubated for another 5 minutes and centrifuged at 500 g for 5 minutes. Then, samples were acquired on a Navios Ex flow cytometer (Beckman Coulter, Brea, CA) equipped with three laser lines and analyzed with the Kaluza software package (Beckman Coulter).

Intracellular stainings were performed as described previously [1]. Briefly, 100 µl of washed EDTA-anticoagulated blood was incubated with 2 ml of BD Pharm Lyse (Becton Dickinson, Franklin Lakes, NJ, USA) for 10 minutes and washed with PBS+0.5% BSA and 0.05% NaN_3. Afterwards, optimal concentrations of the antibodies listed in **Table S1** for surface staining were incubated for 15 minutes and washed with PBS+0.5% BSA and 0.05% NaN_3. Subsequently 100 µl of 1:4 diluted Fixation concentrate with Perm diluent (Thermo Fischer Scientific, Waltham, MA, USA) was added to the samples and incubated for 30 minutes, subsequently the samples were washed with 2 ml of permeabilization buffer. For intracellular staining, optimal concentrations of anti-Foxp-3 and anti-Helios mAbs were added for 30 minutes and samples were washed once with 2 ml of permeabilization buffer and once with 4.5 ml of permeabilization buffer. After the staining procedure, samples were acquired on a Navios Ex flow cytometer (Beckman Coulter, Brea, CA) equipped with three laser lines and analyzed with the Kaluza software package (Beckman Coulter).

Real-time PCR assessment of TRECs and KRECs

DNA was isolated from peripheral blood leukocytes using a Maxwell 16 DNA extraction device (Promega Corporation, Madison, WI) according to the manufacturer's instructions. The quantity of TRECs and KRECs was assessed by real-time PCR (in-house validated using control collectives of different age (newborns, their mothers, penta- and heptagenarians) performed on a QuantStudio 6 Real-Time PCR System (Applied Biosystems, Waltham, MA), with an. In brief, 1.25 µl of a DNA solution (concentration ranges between 25 and 70 ng per µl) were incubated in a mastermix (TaqMan Universal PCR Master Mix, Thermo Fisher Scientific, Waltham, MA), together with oligonucleotide primers and probes in a final volume of 25 µl. Probes were labelled at 5-' and 3'-ends with the fluorescent dyes 6FAM or TAMRA. Reactions were setup in triplicates. Primer-probe combinations [2] were used to detect T cell receptor excision circles (forward primer 5'-CAC ATC CCT TTC AAC CAT GCT-3', reverse primer 5'-TGC AGG TGC CTA TGC ATC A-3', and probe 5'-ACA CCT CTG GTT TTT GTA AAG GTG CCC ACT-3'), kappa-deleting recombination excision circles (forward primer 5'-TCC CTT AGT GGC ATT ATT TGT ATC ACT-3', reverse primer 5'-AGG AGC CAG CTC TTA CCCTAG AGT-3', and probe 5'- TCT GCA CGG GCA GCA GGT TGG-3') or the reference TR alpha constant gene (TRAC) (forward primer 5'-TGG CCT AAC CCT GAT CCT CTT-3', reverse primer 5'-GGA TTT AGA GTC TCT CAG CTG GTA CAC-3', and probe 5'-TCC CAC AGA TAT CCA GAA CCC TGA CCC-3'). PCR started with an initial incubation at 95 °C for eight minutes followed by 60 cycles of denaturation at 95 °C for 15 seconds annealing at 55 °C for 30 seconds and extension at 72 °C for 30 seconds. The threshold cycles (Ct-values) as reported by the machine were edited manually if necessary. The median Ct-value of each triplicate was used as relative

measure of the concentration of the respective amplification product. The difference between the Ct-values of the TRAC gene and the Ct-values of the excision circle genes was used to calculate the number of excision circle containing cells per $1x10^5$ $CD3^+$ or $CD19^+$ lymphocytes, respectively, using the formula: $1 \times 10^5 \times 2^{Ct\text{-}reference+1-Ct\text{-}target} \times subpop^{-1}$, where Ct-reference denotes the threshold cycle of the reference (TRACs) amplification, Ct-target denotes the threshold cycle of either TRECs or KRECS amplification, respectively; subpop indicates the fraction of either $CD3^+$ or $CD19^+$ lymphocytes in comparison to all leukocytes. For the TRAC gene a correction of an additional cycle was applied to accommodate for the two copies present in either $CD3^+$ or $CD19^+$ lymphocytes. Data obtained with TRECs and KRECs analyses significantly correlated with numbers of RTE (positively, $p = 4.2 \times 10^{-15}$) or memory T cells (negatively, $p = 2.4 \times 10^{-6}$) and naive (positively, $p = 4.3 \times 10^{-7}$) or memory B cells (negatively, $p = 5.4 \times 10^{-7}$), respectively.

Determination of SARS-CoV-2-specific serum antibodies

SARS-CoV-2 antibody titers were analyzed as previously described [9] with the following modifications. IgG responses to SARS-CoV-2 S protein and the receptor binding domain (RBD) were determined by ELISA. SARS-CoV-2 S protein (Genscript, Piscataway, NJ, USA) and RBD (GenScript) were coated at 2 µg/ml in bicarbonate buffer onto NUNC Maxisorb 96 well plates (Thermofisher, Thermo-Fisher Scientific, Waltham, MA, USA) at room temperature for 5 hours. Plates were washed 3 times with washing buffer (PBS, 0.05% Tween 20) and subsequently blocked with blocking buffer (PBS, 0.05% Tween 20, 2% BSA) over night. Serum samples 1:40 diluted were applied and incubated at 4°C overnight. To determine human IgG reactivity, plates were washed 3 times and incubated with 1: 1000 diluted HRP-conjugated anti-human IgG (BD, San Jose, CA, USA) for 1 hour. After washing 3

126 times, the plates were developed with ABTS (Sigma-Aldrich, St. Louis, MO, USA) for
127 colorimetric detection of bound antibodies and optical density was measured at
128 405/492 nm with an Infinite F50 ELISA reader (Tecan, Männedorf, Switzerland).
129 In addition, total antibodies against the SARS-CoV-2 nucleocapsid (N) antigen were
130 measured with the Elecsys® Anti-SARS-CoV-2 assay (Roche Diagnostics, Rotkreuz,
131 Switzerland) on a Cobas e 801 modular analyzer (Roche Diagnostics, Rotkreuz,
132 Switzerland) as described previously [34].
133
134 **Statistical analyses**
135 We assessed variables potentially associated with COVID-19 disease. To test the H_0
136 of no association with the outcome univariate analysis of differences between
137 COVID-19 patients and healthy subjects was carried out with the Mann-Whitney-U-
138 test due to outliers and skewness of some variables.
139 Multivariate logistic regression analyses were performed for the 46 blood cell and
140 serum parameters, which indicated significant differences in the univariate analyses.
141 For that purpose, forward stepwise logistic regression by Wald's statistic
142 (Nagelkerkes R^2=0,572, Omnibus-Test $p<0.001$) was performed and additional
143 parameters were included as long as $p<0.05$. Principal component analyses (PCA)
144 were performed using clinical parameters and by applying Bartlett's test of sphericity.
145 For data management MS Excel was used. Data were calculated using the SPSS
146 Version 17.0 (IBM, New York, NY) and the GraphPad 6.0 software (GraphPad
147 Software Inc., La Jolla, CA), respectively.
148

SUPPLEMENTAL REFERENCES

1. Kohler C, Smole U, Kratzer B, Trapin D, Schmetterer KG, Pickl WF. Allergen alters IL-2/alphaIL-2-based Treg expansion but not tolerance induction in an allergen-specific mouse model. *Allergy.* 2020;75(7):1618-1629.
2. Sottini A, Ghidini C, Zanotti C, et al. Simultaneous quantification of recent thymic T-cell and bone marrow B-cell emigrants in patients with primary immunodeficiency undergone to stem cell transplantation. *Clin Immunol.* 2010;136(2):217-227.

SUPPLEMENTAL FIGURE AND TABLE LEGENDS

TABLE S1. List of monoclonal antibodies used in this study.

TABLE S2. List of regular medications taken by COVID-19 convalescent patients and healthy control subjects

TABLE S3. Significant differences in leukocyte populations between COVID-19 convalescent patients and healthy control subjects.

TABLE S4. Significant differences in T lymphocyte subpopulations between COVID-19 convalescent patients and healthy control subjects.

TABLE S5. Significant differences in B lymphocyte subpopulations between COVID-19 convalescent patients and healthy control subjects.

FIGURE S1. Impact of primary SARS-CoV-2 infection on absolute counts of leukocyte subpopulations as determined 10 weeks after disease onset. Shown are relative values of the indicated leukocyte populations in peripheral blood of healthy control subjects (HC) and COVID-19 convalescent patients (COVID-19). Bars show mean values, whiskers the standard deviation, and open circles the values of single individuals. Data show pooled results of daily stainings (whole blood, 6-9 individuals per day) of n=98 for HC, and n=109 for COVID-19 patients, except for panels determining HLA-DR expression where n=97 for HC. P-values were determined by Mann-Whitney U-test and are indicated.

FIGURE S2. Primary SARS-CoV-2 infection leads to significant and sustained activation of $CD3^+CD8^+$ T Lymphocytes**.** Shown are representative two-parameter contour blots of a healthy control subject and a COVID-19 convalescent patient stained for CD3, CD4 and CD8 (shown on the x-axis, respectively) and HLA-DR (y-axis). Makers were set according to negative lymphoid cell populations. Numbers indicate percent cell within the respective quadrant.

FIGURE S3. Impact of primary SARS-CoV-2 infection on absolute amounts of T cell subpopulations levels as determined 10 weeks after disease onset. Shown are the relative values of selected T cell subpopulations in PB of healthy control subjects (HC) and COVID-19 convalescent patients (COVID-19). Bars show mean values, whiskers the standard deviation, and open circles the values of single individuals. Data show pooled results of daily stainings (whole blood, 5-9 individuals per day) of n=98 for HC, and n=109 for COVID-19 patients, except for panels determining CD25/Foxp3 n=97 for HC; and CD45RO/CCR7 n=95 for HC and n=105 for COVID-19. P-values were determined by Mann-Whitney U-test and are indicated.

FIGURE S4. Primary SARS-CoV-2 infection significantly increases the number of $CD4^+CD127^+$ and of $CD3^+CD8^+CD45RA^-CD45RO^+CCR7^+$ T Lymphocytes. **A)** Shown are representative two-parameter contour blots of a healthy control subject and a COVID-19 convalescent patient stained for CD3, CD4 (gate), CD25 or CD45RA (x-axis) and CD127 (y-axis). Makers were set according to negative lymphoid cell

populations. **B)** Shown are two-parameter contour blots of a representative healthy donor and a representative COVID-19 convalescent individual stained for CD3, CD8 (gate), CD45RA or CCR7 (x-axis) and CD45RO (y-axis). Makers were set according to negative lymphoid cell populations. Numbers indicate percent cell within the respective quadrant.

FIGURE S5. Frequency of CD27 and CD28 expression on CD3+CD8+CD45RO+CCR7+ memory T cells. Shown are the mean frequencies of CD27 and/or CD28 expression on cytotoxic memory T cells of COVID-19 convalescent patients (black bars) as compared to healthy control subjects (white bars). Whiskers show the standard deviation. *, $P < 0.05$ as determined by ANOVA

FIGURE S6. Impact of primary SARS-CoV-2 infection on absolut amounts of B cell subpopulations as determined 10 weeks after disease onset. Shown are the relative values of the indicated B cell sub populations in PB of healthy control subjects (HC) and COVID-19 convalescent patients (COVID-19). Bars show mean values, whiskers the standard deviation, and open circles the values of single individuals. Data show pooled results of daily stainings (whole blood, 5-9 individuals per day) of n=78 for HC, and n=108 for COVID-19 patients. P-values were determined by Mann-Whitney U-test and are indicated.

FIGURE S7. Primary SARS-CoV-2 infection leads to significant and sustained increases of both transitional B cells and plasmablasts. Shown are representative two-parameter contour blots of a healthy control subject and a COVID-19

231 convalescent patients stained for CD19 (gate) and CD38 (x-axis) and surface IgM (y-
232 axis). Makers were set according to negative lymphoid cell populations. Numbers
233 indicate percent cell within the respective quadrant.

234

235 **FIGURE S8.** ROC statistics of blood parameters. This subset model is the result of
236 forward stepwise logistic regression by Wald's statistic (Nagelkerkes R^2=0,572,
237 Omnibus-Test p<0.000). Additional parameters were included as long as $p < 0.05$.

238

239

240 **TABLE S1. List of monoclonal antibodies used for flow cytometry for analyses of cell surface and intracellular antigens.**

Specificity	Clone Name	Species	Fluorophore	Source
CD8	RPA-T8	Mouse IgG1	FITC	Thermo Fisher Scientific, Waltham, MA, USA
sIgK	TB28-2	Mouse IgG1	FITC	Thermo Fisher Scientific
TCR a/b	WT31	Mouse IgG1	PE	Thermo Fisher Scientific
CD19	HIB19	Mouse IgG1	PE-eFluor610	Thermo Fisher Scientific
CD4	RPA-T4	Mouse IgG1	PE-eFluor610	Thermo Fisher Scientific
CD33	WM-53	Mouse IgG1	PerCP-Cy5.5	Thermo Fisher Scientific
CD3	UCHT1	Mouse IgG1	PE-Cy7	Thermo Fisher Scientific
CD5	L17F12	Mouse IgG2a	APC	Thermo Fisher Scientific
CD20	2H7	Mouse IgG2b	AF700	Thermo Fisher Scientific
CD38	HIT2	Mouse IgG1	APC-eFluor780	Thermo Fisher Scientific
HLA-DR	LN3	Mouse IgG2b	eFluor450	Thermo Fisher Scientific
CD45	HI30	Mouse IgG1	eFluor506	Thermo Fisher Scientific
sIgD	IA6-2	Mouse IgG2a	FITC	Thermo Fisher Scientific
CD21	HB5	Mouse IgG2a	PE	Thermo Fisher Scientific
CD10	SN5c	Mouse IgG1	PerCP-eFluor710	Thermo Fisher Scientific
CD27	O323	Mouse IgG1	PE-Cy7	Thermo Fisher Scientific
CD24	eBioSN3 (SN3 A5-2H10)	Mouse IgG1	APC	Thermo Fisher Scientific

sIgM	SA-DA4	Mouse IgG1	eFluor450	Thermo Fisher Scientific
CD27	O323	Mouse IgG1	FITC	Biolegend, San Diego, CA, USA
CD62L	SK11	Mouse IgG2a	PE	Becton Dickinson, Franklin Lakes, NJ, USA
CD45RO	UCHL1	Mouse IgG2a	PerCP-eFluor710	Thermo Fisher Scientific
CD197 (CCR7)	3D12	Rat IgG2a	APC	Thermo Fisher Scientific
CD45RA	HI100	Mouse IgG2b	AF700	Biolegend
CD28	CD28.2	Mouse IgG1	APC-eFluor780	Thermo Fisher Scientific
CD8	RPA-T8	Mouse IgG1	eFluor450	Thermo Fisher Scientific
CD31	WM-59	Mouse IgG1	BV510	Becton Dickinson
Foxp3	PCH101	Rat IgG2a	FITC	Thermo Fisher Scientific
CD127	eBioRDR5	Mouse IgG1	PE	Thermo Fisher Scientific
CD25	CD25-4E3	Mouse IgG2b	PerCP-eFluor710	Thermo Fisher Scientific,
Helios	22F6	Hamster IgG	APC	Thermo Fisher Scientific
CD73	AD2	Mouse IgG1	APC-eFluor780	Thermo Fisher Scientific
CD39	eBioA1	Mouse IgG1	Super Bright 436	Thermo Fisher Scientific

241

242 Table shows the specificity, clone names, species and supplier (source) of the respective monoclonal antibodies and their conjugation

243 with the respective fluorophores used in this study.

244 **TABLE S2. List of drugs reported by the patients**

Drug	COVID-19 convalescent patients (n=108)	Healthy control subjects (n=98)
abacavir, dolutegravir, lamivudine	1	0
acetylsalicylic acid	9	3
allopurinol	0	1
amiodarone	1	0
amlodipine	5	3
apixaban	1	0
atorvastatin	3	2
atovaquone	1	0
beclomethasone dipropionate	0	1
bisoprolol	5	1
budesonide	2	3
Ca^{2+}; vitamin D3	1	0
cabergoline	0	1
candesartan	5	5
cyclosporine	1	0
dabigatran	0	1
daflon	1	0
dapagliflozin	1	0
desloratadine	1	1
diosmin	0	1
doxazosin	1	0
edoxaban	1	0
empagliflozin	1	0
enalapril	1	3
erenumab	1	0
escitalopram	0	1
esomeprazole	1	1
estradiol	0	1

estriol	0	1
ethinylestradiol	1	2
ezetimibe	1	0
famotidine	1	0
fenofibrate	1	0
fexofenadine	1	0
finasteride	1	0
fluoxetine	0	1
fluticasone	0	1
fluvoxamine	0	1
formoterol	3	4
guanfacine	1	0
hydrochlorothiazide	2	2
ibandronic acid	0	1
imidapril	0	1
insulin	1	0
irbesartan	1	0
Iron(II)fumarate	2	0
lamotrigine	1	0
hydrochloride lercanidipine	1	1
levocetirizine, cetirizine-AD6C	0	3
levonorgestrel	0	1
levothyroxine	12	13
linagliptin	1	0
lipase-, amylase-, protease-mix	0	1
lisinopril	3	1
magnesium	1	0
mefenamic acid	0	1
metamizole	2	1
metformin	2	1
methylphenidate	0	1

methylprednisolone	2	1
metoprolol	2	0
montelukast	3	1
naproxen	1	0
nebivolol	2	1
olodaterol	0	1
pantoprazol	1	2
paroxetine	1	0
phenoxymethylpenicillin	1	0
phenprocoumon	0	1
pregabalin	1	1
ramipril	2	0
rilmenidine	1	0
rosuvastatin	2	2
salmeterol	0	1
sertraline	1	2
simvastatin	2	1
tamsulosin	4	0
terazosin	1	0
testosterone	0	1
tiotropium bromide	0	1
tramadol	0	1
trazodone	2	0
triazolam	1	0
trimetazidine	1	0
valsartan	3	1
venlafaxine	1	1
verapamil	1	0
vitamin B9 folic acid	1	0
vitamin D3	3	3
zolpidem	1	0

245

246 Shown are the numbers of patients and control subjects taking the indicated drugs

247 **TABLE S3. Significant differences in leukocyte populations between COVID-19 convalescent patients and healthy control**

248 **subjects.**

	COVID-19 convalescent patients (n=109) (absolute counts)	Healthy control subjects (n=98) (absolute counts)	P COVID-19 vs HC	COVID-19 convalescent patients (n=109) (relative values)	Healthy control subjects (n=98) (relative values)	P COVID-19 vs HC
Leukocytes	6,384±1.677(*	7,006±1,961	0.0156(§			
Granulocytes	4,111±1,477	4,693±1,588	0.0033	63.31±9.39	66.40±8.77	0.0239
Monocytes	478±159	468±207	0.5190	7.63±2.17	6.70±2.14	0.0177
Lymphocytes	1,809±571	1,857±622	0.5449	29.10±8.22	27.08±7.71	0.0590
CD3+ T cells	1,324±461	1,338±472	0.8162	72.47±7.93	71.84±7.11	0.4529
CD3+TCR ab+ T cells	1248±440	1258±449	0.8781	68.31±7.85	67.50±7.15	0.3406
CD3+ TCR gd+ T cells	69±70	69±65	0.7369	3.79±3.58	3.65±3.24	0.8487
CD3+CD4+ T cells	807±291	846±332	0.5411	44.65±8.55	45.46±7.78	0.6100
CD3+CD8+ T cells	428±242	402±195	0.7573	22.98±8.65	21.61±7.11	0.3574
CD4/CD8-Ratio	2.32±1.18	2.46±1.33	0.4349			
CD3+CD4+CD8+ DP T cells	19±32	19±34	0.2969	0.98±1.37	0.98±1.46	0.4424
CD3+TCR ab+ CD4-CD8-	22±19	23±22	0.6089	1.77±1.46	1.92±1.58	0.5303

T cells						
CD3+HLA-DR+ T cells	107±85	81±54	0.0248	5.78±3.84	4.34±2.50	0.0054
CD3+CD4+HLA-DR+ T cells	33±18	31±19	0.3630	1.88±0.93	1.70±0.87	0.1921
CD3+CD8+HLA-DR+ T cells	61±65	38±34	0.0079	3.21±2.91	2.05±1.61	0.0014
CD3+HLA-DR+CD38+ T cells	4.6±3.6	3.5±2.7	0.0275	0.27±0.24	0.19±0.14	0.0051
CD3+CD4+HLA-DR+CD38+ T cells	2.1±1.6	1.6±1.2	0.0605	0.12±0.12	0.09±0.06	0.0210
CD3+CD8+HLA-DR+CD38+ T cells	1.5±1.7	1.0±1.2	0.0473	0.09±1.06	0.05±0.07	0.0178
CD19+ B cells	175±83	187±99	0.6873	9.69±3.32	10.03±3.62	0.6787
CD3-CD56+ NK cells	251±124	261±144	0.9870	14.46±7.52	14.17±6.21	0.9842
CD3+CD56+ NKT cells	8±11	8±14	0.4376	0.39±0.46	0.43±0.59	1.0000

249

250 *) x 10^6 cells/L as mean ± standard deviation

251 §) significant P-values are shown in red font

252 **TABLE S4. Significant differences in T lymphocyte subpopulations between COVID-19 convalescent patients and healthy**
253 **control subjects.**

	COVID-19 convalescent patients (n=109) (absolute counts)	Healthy control subjects (n=98) (absolute counts)	P COVID-19 vs HC	COVID-19 convalescent patients (n=109) (relative values)	Healthy control subjects (n=98) (relative values)	P COVID-19 vs HC
CD45RA+CD62L+CD31+ RTE in CD3+ T cells	227±157	256±199	0.3222	16.85±10.35	19.11±11.13	0.1351
CD4+CD45RA+CD62L+CD31+ RTE in CD3+CD4+ T cells	141±103	165±126	0.2078	17.01±10.85	18.40±10.27	0.2215
CD8+CD45RA+CD62L+CD31+ RTE in CD3+CD8+ T cells	86±70	100±95	0.5770	20.81±13.78	23.73±16.64	0.3592
CD127+ in CD3+CD4+ T cells	498±226	370±248	<0.0001	62.44±17.69	44.83±24.22	<0.0001
CD45RA+ naive T cells in CD3+ T cells	479±271	539±279	0.0543	35.35±12.80	38.89±12.19	0.0350
CD25+ in CD3+ T cells	14±14	12±8	0.0872	1.12±0.92	0.90±0.65	0.0284
CD4+CD45RA+ naive T cells in CD3+ T cells	226±139	282±188	0.0309	17.00±8.34	20.21±9.32	0.0128
CD45RA+CCR7+ in CD3+CD4+ T cells	259±145	304±207	0.2283	31.00±12.70	33.83±12.82	0.1707

CD45RO-CCR7+ in CD3+CD4+ T cells	317±189	371±242	0.1577	37.77±14.57	41.03±13.18	0.1206
CD45RA+CCR7- in CD3+CD4+ T cells	43±42	59±72	0.2527	5.46±5.03	7.09±7.69	0.2462
CD45RO-CCR7- in CD3+CD4+ T cells	86±66	107±77	0.0150	11.35±10.79	12.66±7.11	0.0171
CD4+CD27+CD28+CCR7+CD45RA+ in CD3+CD4+ naïve T cells	220±140	261±187	0.2108	26.15±11.78	28.67±11.56	0.1372
CD127+CD45RA+ in CD3+CD4+ T cells	137±114	79±106	<0.0001	24.47±13.68	15.66±13.79	<0.0001
CD127-CD25+ in CD3+CD4+ T cells	39±27	38±22	0.6962	4.75±2.30	4.53±1.77	0.7230
CD8+CD45RA+ T cells in CD3+ T cells	225±173	225±136	0.4041	16.24±8.57	16.93±7.41	0.5365
CD45RA+CCR7+ in CD3+CD8+ T cells	83±67	101±89	0.1465	20.85±14.14	24.81±14.85	0.0633
CD45RO-CCR7+ in CD3+CD8+ T cells	85±66	108±92	0.0704	21.52±13.91	26.60±15.13	0.0145
CD45RA+CCR7- in CD3+CD8+ T cells	123±14	102±88	0.8420	25.35±14.74	24.70±14.95	0.7311
CD45RO-CCR7- in CD3+CD8+ T cells	195±184	175±136	0.8804	41.98±17.28	42.35±16.75	0.7973
CD8+CD27+CD28+CCR7+CD45RA+ naïve cells in CD3+CD8+ T cells	75±80	59±55	0.1952	16.93±11.44	14.71±10.81	0.1650
CD45RO+ memory T cells in CD3+ T cells	563±248	505±211	0.1178	43.53±13.00	39.26±12.68	0.0135
CD4+CD45RO+ memory T cells in CD3+ T cells	418±178	389±164	0.3109	32.56±10.15	30.23±9.63	0.0978
CD45RO+CCR7- in CD3+CD4+ T cells	251±129	221±88	0.1465	32.07±11.75	28.13±9.94	0.0075
CD45RA-CCR7- in CD3+CD4+ T cells	309±146	286±122	0.3431	39.47±13.17	35.84±12.05	0.0753
CD4+CD27+CD28+CCR7+CD45RA- AE1 cells in CD3+CD4+ T cells	175±94	180±111	0.8343	21.55±7.27	20.97±8.62	0.5200

CD4+CD27+CD28+CCR7-CD45RA- AE2 cells in CD3+CD4+ T cells	219±10	206±92	0.5368	27.75±9.56	25.79±9.01	0.1910
CD8+CD45RO+ T cells in CD3+ T cells	113±79	87±54	0.0263	8.58±4.67	6.82±3.88	0.0045
CD45RO+CCR7- in CD3+CD8+ T cells	128±89	99±55	0.0502	32.42±14.65	26.90±11.11	0.0052
CD45RA-CCR7- in CD3+CD8+ T cells	203±122	179±103	0.1695	49.80±15.14	46.23±15.05	0.1468
CD8+CD27+CD28+CCR7+CD45RA- AE1 cells in CD3+CD8+ T cells	15±20	10±10	0.0572	3.38±2.96	2.60±1.71	0.0974
CD8+CD27+CD28+CCR7-CD45RA- AE2 cells in CD3+CD8+ T cells	103±70	98±65	0.7532	24.36±10.17	25.34±10.77	0.5862
CD45RO+CCR7+ in CD3+CD4+ T cells	152±86	149±83	0.7109	18.81±7.69	18.18±8.47	0.2024
CD45RA-CCR7+ in CD3+CD4+ T cells	194±102	199±121	0.7944	24.07±8.23	23.23±9.38	0.4818
CD4+CD27-CD28+CCR7-CD45RA-/+ AE3 cells in CD3+CD4+ T cells	47±33	41±22	0.3406	6.05±3.40	5.12±2.53	0.0822
CD4+CD27-CD28-CCR7-CD45RA-/+ AE4 cells in CD3+CD4+ T cells	19±36	12±15	0.0912	2.47±3.91	1.57±2.01	0.0769
CD45RO+CCR7+ in CD3+CD8+ T cells	15±14	15±10	0.7532	4.08±3.06	4.14±3.21	0.9094
CD45RA-CCR7+ in CD3+CD8+ T cells	16±16	15±12	0.7440	4.00±3.02	4.26±3.83	0.7292
CD8+CD27+CD28-CCR7-CD45RA-/+ AE3 cells in CD3+CD8+ T cells	67±51	69±43	0.3686	15.68±7.31	18.15±8.99	0.0437
CD8+CD27-CD28-CCR7-CD45RA-/+ AE4 cells in CD3+CD8+ T cells	57±58	66±83	0.8554	13.83±10.97	15.17±12.70	0.6126
CD8+CD27-CD28-CCR7-CD45RA+ TEMRA	28±29	33±47	0.6464	6.73±5.84	6.64±8.07	0.9201

in CD3+CD8+ T cells						
Foxp3+ in CD3+CD4+ CD127-CD25+T cells	11±15	15±11	0.0004	27.73±25.70	42.10±27.26	0.0001
Foxp3+CD39+ in CD3+CD4+ CD127-CD25+T cells	8±13	10±9	0.0053	19.84±20.02	29.01±22.83	0.0012
Foxp3+CD73+ in CD3+CD4+ CD127-CD25+T cells	1.5±1.9	3.1±3.3	<0.0001	3.45±3.84	7.69±6.88	<0.0001
Foxp3+Helios+ in CD3+CD4+ CD127-CD25+T cells	8±13	10±8	0.0006	19.95±20.08	29.30±21.80	0.0011
Foxp3+CD45RA+ in CD3+CD4+ CD127-CD25+T cells	4±6	6±6	0.0023	11.18±11.07	16.17±13.85	0.0019

254

255 *) x 10^6 cells/L as mean ± standard deviation

256 §) significant P-values are shown in red font

257 TEMRA T effector memory CD45RA$^+$ T cells

258 AE antigen experienced T cells according to *Appay et al.* [37]

259
260

TABLE S5. Significant differences in B lymphocyte subpopulations between COVID-19 convalescent patients and healthy control subjects.

	COVID-19 convalescent patients (n=109) (absolute counts)(*	Healthy control subjects (n=98) (absolute counts)	P COVID-19 vs HC	COVID-19 convalescent patients (n=109) (relative values)	Healthy control subjects (n=98) (relative values)	P COVID-19 vs HC
CD20+ B cells($	170±83	180±98	0.8504	9.36±3.34	9.60±3.56	0.8522
CD5+ B cells	41±32	37±34	0.2374	2.25±1.61	2.02±1.68	0.1437
Ig kappa+ B cells	98±47	107±59	0.6122	5.42±1.91	5.68±2.26	0.6920
Ig lambda+ B cells	77±38	80±42	0.8893	4.24±1.52	4.28±1.62	0.9840
CD21- B cells	16±10	19±14	0.2397	9.87±4.41	10.23±5.95	0.7551
CD21-CD10+ immature B cells	<0±0	<0±0	0.2087	0.26±0.29	0.29±0.29	0.4330
IgM+CD38+ transitional B cells	8±6	7±5	0.0425($	5.00±3.07	3.57±2.30	0.0020
CD21+CD27- naive B cells	111±61	128±76	0.1871	62.71±12.80	62.95±13.26	0.8891
CD21+CD27+ memory B cells	47±31	51±33	0.4348	27.43±10.33	26.82±10.45	0.7228
CD21+CD27+IgD+IgM+ non-switched memory B cells	26±19	28±21	0.5401	15.13±7.16	14.73±6.85	0.7053
CD21+CD27+IgD-IgM- switched memory B cells	19±15	20±16	0.5059	11.07±5.71	10.52±5.80	0.3937

CD21lowCD38low activated B cells	7±6	9±10	0.1719	4.34±2.45	4.90±3.91	0.8028
IgM-CD38+ plasmablasts	2.5±1.8	1.6±1.3	0.0015	1.56±0.97	1.04±0.95	<0.0001

263

264 $) gated on CD19+ cells

265 *) x 10^6 cells/L as mean ± standard deviation

266 §) significant P-values are shown in red font

267
268